bioRxiv preprint doi: https://doi.org/10.1101/2020.07.26.221937; this version posted July 26, 2020. The copyright holder for this preprint (which was not certified by peer review) is the author/funder. All rights reserved. No reuse allowed without permission.

Quorum Sensing Regulates 'swim-or-stick' Lifestyle in the Phycosphere

Cong Fei[1], Michael A. Ochsenkühn[1], Ahmed A. Shibl[1], Ashley Isaac[1], Changhai Wang[2], Shady A. Amin[1*]

[1]Marine Microbial Ecology Lab, Biology Program, New York University Abu Dhabi, Abu Dhabi, United Arab Emirates

[2]College of Resources and Environmental Science, Nanjing Agriculture University, Nanjing, China

[*]**Corresponding author:** Dr. Shady. A. Amin, Marine Microbial Ecology Lab, Biology Program, New York University Abu Dhabi, Abu Dhabi, United Arab Emirates. E-mail: samin@nyu.edu (SAA), +971 2 628 5743, PO Box 129188, NYU Abu Dhabi, Abu Dhabi, UAE.

Running title: Quorum Sensing in the Phycosphere.

Originality-significance statement

Motility and biofilm formation are processes regulated by quorum sensing (QS) in bacteria. Both functions are believed to play an important role in interactions between bacteria and phytoplankton. Here, we show that two bacterial symbionts from the microbial community associated with a ubiquitous diatom switch their motile lifestyle to attached cells while an opportunist bacterium from the same community is incapable of attachment, despite possessing the genetic machinery to do so. Further work indicated that the opportunist lacks QS signal synthases while the symbionts produce three QS signals, one of which is mainly responsible for regulating symbiont colonization of the diatom microenvironment. These findings suggest that QS regulates colonization of diatom surfaces and further work on these model systems will inform our

bioRxiv preprint doi: https://doi.org/10.1101/2020.07.26.221937; this version posted July 26, 2020. The copyright holder for this preprint (which was not certified by peer review) is the author/funder. All rights reserved. No reuse allowed without permission.

understanding of particle aggregation and bacterial attachment to marine snow and how these processes influence the global carbon cycle.

Summary

Interactions between phytoplankton and bacteria play major roles in global biogeochemical cycles and oceanic nutrient fluxes. These interactions occur in the microenvironment surrounding phytoplankton cells, known as the phycosphere. Bacteria in the phycosphere use either chemotaxis or attachment to benefit from algal excretions. Both processes are regulated by quorum sensing (QS), a cell-cell signaling mechanism that uses small infochemicals to coordinate bacterial gene expression. However, the role of QS in regulating bacterial attachment in the phycosphere is not clear. Here, we isolated a *Sulfitobacter pseudonitzschiae* F5 and a *Phaeobacter* sp. F10 belonging to the marine *Roseobacter* group and an *Alteromonas macleodii* F12 belonging to Alteromonadaceae, from the microbial community of the ubiquitous diatom *Asterionellopsis glacialis*. We show that only the *Roseobacter* group isolates (diatom symbionts) can attach to diatom transparent exopolymeric particles. Despite all three bacteria possessing genes involved in motility, chemotaxis, and attachment, only *S. pseudonitzschiae* F5 and *Phaeobacter* sp. F10 possessed complete QS systems and could synthesize QS signals. Using UHPLC-MS/MS, we identified three QS molecules produced by both bacteria of which only 3-oxo-$C_{16:1}$-HSL strongly inhibited bacterial motility and stimulated attachment in the phycosphere. These findings suggest that QS signals enable colonization of the phycosphere by algal symbionts.

Keywords: quorum sensing; diatoms; *Roseobacter* group; phycosphere

bioRxiv preprint doi: https://doi.org/10.1101/2020.07.26.221937; this version posted July 26, 2020. The copyright holder for this preprint (which was not certified by peer review) is the author/funder. All rights reserved. No reuse allowed without permission.

Introduction

Phytoplankton constitute the foundation of the marine food web as they are responsible for nearly half of primary production on Earth (Field et al., 1998). Through their ability to carry out photosynthesis, phytoplankton transform atmospheric carbon dioxide gas to organic matter (Simon et al., 2009) that is assimilated and remineralized by heterotrophic bacteria (Pomeroy, 1974; Burkhardt et al., 2014). In exchange, bacteria produce essential factors (e.g., vitamins) (Kazamia et al., 2012; Bertrand et al., 2015) to support the growth of phytoplankton (Amin et al., 2012). Cumulatively, phytoplankton-bacteria symbiosis is believed to play an important role in nutrient availability and major biogeochemical cycles (Buchan et al., 2014; Durham et al., 2019).

Several bacterial lineages have been consistently observed to co-occur with phytoplankton, such as members of the *Roseobacter* group, Gammaproteobacteria, and Flavobacteria (Wagner-Döbler and Biebl, 2006; Teeling et al., 2012). Particularly, members of the *Roseobacter* group (hereafter roseobacters) have been shown consistently to form symbiotic relationships with phytoplankton (Amin et al., 2012). For example, roseobacters are adept at acquiring and assimilating phytoplankton metabolites (Miller et al., 2004) in exchange for a variety of cofactors. *Ruegeria pomeroyi* has been shown to assimilate organic sulfur compounds from the diatom *Thalassiosira pseudonana* in exchange for production of cobalamin, which is required for diatom growth (Durham et al., 2015). *Sulfitobacter pseudonitzschiae* SA11 produces the hormone indole-3-acetic acid (IAA) to enhance cell division of the diatom *Pseudo-nitzschia multiseries*, which leads to an increase in carbon export by the diatom and the exchange of diatom-derived organosulfur compounds and bacterial ammonia (Amin et al., 2015). Other phytoplankton such as the coccolithophore, *Emiliania huxleyi*, display different morphologies in response to endogenous IAA (Labeeuw et al., 2016) and exhibit enhanced cell division by roseobacters-derived IAA (Segev et al., 2016; Bramucci et al., 2018). IAA is an endogenous hormone that regulates plant differentiation and is also produced and excreted by

bioRxiv preprint doi: https://doi.org/10.1101/2020.07.26.221937; this version posted July 26, 2020. The copyright holder for this preprint (which was not certified by peer review) is the author/funder. All rights reserved. No reuse allowed without permission.

plant symbionts and some plant pathogens to interfere with plant root differentiation (Spaepen et al., 2007; Spaepen and Vanderleyden, 2011). Although eukaryotic phytoplankton like diatoms and coccolithophores are unicellular and do not undergo differentiation as defined in multicellular eukaryotes, IAA appears to have evolved the ability to manipulate the cell cycle in both groups of organisms, with related bacteria playing an important role in eukaryotic IAA perception in both marine and rhizobial environments (Seymour et al., 2017). A prerequisite for these symbiotic exchanges to occur is the intimate spatial proximity between the phytoplankton host and its symbionts.

Chemical exchanges between bacteria and phytoplankton occur in the microenvironment immediately adjacent to phytoplankton cells, known as the phycosphere (Bell and Mitchell, 1972; Seymour et al., 2017). Phytoplankton continuously exude organic matter, sometimes up to 50% of the cell's total fixed carbon (Thornton, 2014). Consequently, the phycosphere is hypothesized to harbor a significantly higher amount of phytoplankton dissolved organic matter (DOM) relative to bulk seawater due to the exudation of DOM by phytoplankton cells, and due to the negligible effects of turbulence on the diffusion of exudates within the minute phycosphere (Seymour et al., 2017). This buildup of DOM ultimately leads to bacterial attraction and colonization of the phycosphere either via chemotaxis or random encounters with phytoplankton cells (Smriga et al., 2016). Once in the phycosphere, beneficial bacteria that produce metabolites essential to phytoplankton (Mayali et al., 2011) may gain an advantage by switching their free-living, planktonic lifestyle in bulk seawater to a surface-attached state on phytoplankton cells. On the other hand, opportunistic bacteria benefit from phytoplankton-derived DOM without providing apparent benefits to phytoplankton hosts (Mayali and Doucette, 2002). Compared to free-living cells, surface-associated cells have greater access to phytoplankton nutrients and gain protection against toxins, antibiotics, and other environmental stressors by forming a biofilm (Jefferson, 2004; Samo et al., 2018).

bioRxiv preprint doi: https://doi.org/10.1101/2020.07.26.221937; this version posted July 26, 2020. The copyright holder for this preprint (which was not certified by peer review) is the author/funder. All rights reserved. No reuse allowed without permission.

Successful colonization of the phycosphere can be enhanced by specific bacterial genetic traits, including chemotaxis, motility, and attachment to surfaces (Slightom and Buchan, 2009; Raina et al., 2019). Chemotaxis enables bacteria to sense changes in local concentrations of food and regulates motility accordingly. Motile bacteria generally exhibit strong chemotaxis to DOM released from phytoplankton (Miller and Belas, 2004; Miller et al., 2004; Stocker, 2012; Smriga et al., 2016), while motility and flagellar genes appear to be critical for attachment and biofilm development in many roseobacters (Miller and Belas, 2006; Bruhn et al., 2007). In the phycosphere, many bacteria may have a biphasic 'swim-or-stick' lifestyle that enables them to rapidly find food sources while minimizing energy expenditures once the food is located. During the motile phase, bacteria use chemotaxis to locate phytoplankton cells (Seymour et al., 2017). Once in the phycosphere, a 'switch' is turned on, causing a transition of the bacteria to a sessile lifestyle, whose phenotype includes loss of flagella and subsequent biofilm development (Geng and Belas, 2010). Despite our knowledge of bacterial behavior, the mechanisms that regulate bacterial motility and attachment in the phycosphere have not been extensively investigated.

Quorum sensing (QS) is one of the best-studied signaling mechanisms for bacterial cell-to-cell communication. Many bacteria have been shown to carry out QS by secreting small signaling molecules, known as autoinducers, to assess changes in bacterial populations and to coordinate gene expression among a whole population (Waters and Bassler, 2005). In Proteobacteria, the primary class of autoinducers is acyl-homoserine lactones (AHLs), which are synthesized by an autoinducer synthase (LuxI) and perceived by an autoinducer regulator (LuxR) (Case et al., 2008). Bacteria use AHLs to regulate functions that are beneficial to carry out collectively, such as virulence, motility, and biofilm formation (Hammer and Bassler, 2003; Daniels et al., 2004; Antunes et al., 2010). Indeed, several *Roseobacter*-group bacteria use AHLs to regulate motility, virulence, biofilm formation, and nutrient acquisition when associated with marine snow (Gram et al., 2002; Hmelo et al., 2011), red alga (Gardiner et al., 2015), and sponges (Zan et al., 2012). The addition of exogenous AHLs produced by bacterial epibionts to colonies of the cyanobacterium

bioRxiv preprint doi: https://doi.org/10.1101/2020.07.26.221937; this version posted July 26, 2020. The copyright holder for this preprint (which was not certified by peer review) is the author/funder. All rights reserved. No reuse allowed without permission.

111 *Trichodesmium* led to increases in the activity of alkaline phosphatase activity and consequently phosphorus
112 acquisition (Van Mooy et al., 2012). In contrast, the lack of complete QS systems often leads to the inability
113 of bacteria to attach to hosts. For example, a *luxR*-type gene knock-out strain of the *Roseobacter*-group
114 member *Nautella italica* R11 was unable to form biofilms or attach to the red alga *Delisea pulchra*
115 (Gardiner et al., 2015). Despite these examples, there is little direct evidence showing how QS regulates
116 bacteria-phytoplankton interactions or how QS influences inter- and intraspecies interactions and behavior
117 between bacteria within microbial consortia in the phycosphere. In this study, we examine how QS
118 influences bacterial behavior in the phycosphere of the ubiquitous diatom, *Asterionellopsis glacialis*, and
119 whether QS provides an advantage to beneficial bacteria relative to other bacteria. Here we hypothesize
120 that QS regulates motility and attachment of beneficial bacteria, which may enhance their access to
121 phytoplankton nutrients over non-beneficial bacteria.

122 *A. glacialis* is a ubiquitous diatom that has been isolated from every major water body around the world
123 (Korner, 1970; Kaczmarska et al., 2014) and has recently been shown to be one of several abundant and
124 widely distributed groups of diatoms from the Tara Oceans expedition (Malviya et al., 2016). In addition,
125 *A. glacialis* often forms blooms and dense patches worldwide (Karentz and Smayda, 1984; Franco et al.,
126 2016) that are characterized by high DOM secretions (Abreu et al., 2003), making this diatom an ideal
127 model system to examine interactions with bacteria. Here, we characterize AHL molecules produced by
128 bacteria isolated from the phycosphere of *A. glacialis* and examine the influence of these AHLs on the
129 ability of beneficial and opportunistic bacteria to colonize the phycosphere of *A. glacialis.*
130

131 **Results and discussion**

132 **Bacterial attachment and influence on diatom physiology**

bioRxiv preprint doi: https://doi.org/10.1101/2020.07.26.221937; this version posted July 26, 2020. The copyright holder for this preprint (which was not certified by peer review) is the author/funder. All rights reserved. No reuse allowed without permission.

A. glacialis strain A3 (deposited as CCMP3542) was isolated from the Persian Gulf and identified as previously described (Behringer et al., 2018). Axenic *A. glacialis* strain A3 cultures were generated using antibiotics as described previously (Amin et al., 2015). Under optimal growth conditions, we noticed that axenic *A. glacialis* strain A3 mostly existed as single cells or chains with an average of approximately three cells per chain while xenic *A. glacialis* strain A3 at the same cell density (~1.5×10^5 cells/mL) formed longer chains and/or aggregated cells (Supplementary Fig. S1A and S1B). Quantifying the abundance of diatom chains spanning 1-3 cells and >3 cells per chain in axenic and xenic cultures showed that chain length did not change appreciably throughout the growth of axenic cultures with roughly half the population forming >3 cells per chain. In contrast, bacteria significantly increased the abundance of longer diatom chains, with 79.4% of the population forming >3 cells per chain relative to axenic cultures in late-exponential to early-stationary phases (Supplementary Fig. S1C). In diatoms, current evidence suggests that chain length is influenced by increasing CO_2 concentrations (Ramos et al., 2014) and grazing pressure (Amato et al., 2018). The finding that bacteria can influence diatom chain length is novel and consistent with observations that bacteria can influence diatom cell size and morphology (Windler et al., 2014).

Removal of free-living bacteria in xenic *A. glacialis* cultures using gravity filtration through a 3-μm membrane filter and staining filtered diatom and bacterial cells with SYBR Green I showed large aggregates of bacteria on and/or in close proximity to diatom cells (Supplementary Fig. S1D). Further staining of the sample with alcian blue, a dye that stains diatom transparent exopolymeric particles (TEP), showed that bacteria mostly attach to TEP (Supplementary Fig. S1E and S1F), an observation consistent with previous observations (Bar-Zeev et al., 2012). Generating biofilm on algal TEP and/or surfaces is a typical behavior of bacteria in aquatic habitats (Kogure et al., 1981; Bagatini et al., 2014) that can enable them to persist in such environments (Geng and Belas, 2010). Forming biofilm on algal surfaces or algal TEP also protects bacteria against toxins and antibiotics and provides shelter from predation (Carvalho, 2018). For example, bacteria residing in a biofilm can tolerate antimicrobial agents at concentrations 100-1000 times needed to

bioRxiv preprint doi: https://doi.org/10.1101/2020.07.26.221937; this version posted July 26, 2020. The copyright holder for this preprint (which was not certified by peer review) is the author/funder. All rights reserved. No reuse allowed without permission.

kill planktonic cells (Lewis, 2001). In addition, colonizing the phycosphere by attaching to TEP may help bacteria to conserve energy that would otherwise be spent on motility and chemotaxis to remain in proximity of the phycosphere (Seymour et al., 2017).

Bacterial isolation

To examine bacterial attachment and influence on diatom chain length in the phycosphere, three bacterial strains were isolated from xenic *A. glacialis* and characterized based on 16S rRNA sequence identity as *Sulfitobacter pseudonitzschiae* F5 (Rhodobacteraceae; >99% similarity to *S. pseudonitzschiae*), *Phaeobacter* sp. F10 (Rhodobacteraceae; 97% similarity to *Phaeobacter gallaeciensis*) and *Alteromonas macleodii* F12 (Alteromonadaceae; 99% similarity to *A. macleodii*) (Supplementary Fig. S2). The *Roseobacter* group (Rhodobacteraceae) is one of the most important groups of marine bacteria that primarily colonize both biotic (e.g., phytoplankton) and abiotic surfaces (e.g., marine snow) (Gram et al., 2002; Dang et al., 2008), and can comprise up to 25% of the marine bacterial community in some regions (Wagner-Döbler and Biebl, 2006). They have been shown to form a substantial component of the *A. glacialis* microbial consortium based both on 16S rRNA amplicon sequencing (Behringer et al., 2018) and shotgun metagenomics (Shibl et al., 2020). Mining the 16S rRNA sequences of the microbial community of *A. glacialis* recovered after 20 days of isolation from the field (Behringer et al., 2018), we recovered reads that display 100% sequence identity to the 16S rRNA gene of *Phaeobacter* sp. F10 and *A. macleodii* F12 and 99% sequence identity to *S. pseudonitzschiae* F5, indicating our bacterial isolates belong to the natural population of xenic *A. glacialis* and that members of this population persist through time under laboratory culturing conditions.

Co-culture of bacterial isolates with the diatom

bioRxiv preprint doi: https://doi.org/10.1101/2020.07.26.221937; this version posted July 26, 2020. The copyright holder for this preprint (which was not certified by peer review) is the author/funder. All rights reserved. No reuse allowed without permission.

178 To test whether these bacteria attach to *A. glacialis*, co-cultures of each bacterium with the diatom were
179 grown in batch cultures, and growth and attachment of both partners were monitored using microscopy.
180 When co-cultured with *A. macleodii* F12, the specific growth rate (μ) of the diatom did not exhibit
181 significant changes relative to axenic controls (μ_{axenic} = 1.02 ± 0.05 d^{-1}; $\mu_{co\text{-}culture}$ = 1.03 ± 0.02 d^{-1})
182 (Supplementary Fig. S3A). Likewise, the growth of the diatom did not vary significantly when co-cultured
183 with *Phaeobacter* sp. F10 (μ_{axenic} = 0.81 ± 0.02 d^{-1}; $\mu_{co\text{-}culture}$ = 0.84 ± 0.04 d^{-1}) (Supplementary Fig. S3B). In
184 contrast, *A. glacialis* co-cultured with *S. pseudonitzschiae* F5 exhibited a 27.6% increase in μ relative to
185 axenic controls (μ_{axenic} = 0.76 ± 0.03 d^{-1}; $\mu_{co\text{-}culture}$ = 0.97 ± 0.03 d^{-1}) (Supplementary Fig. S3C). In all co-
186 cultures, bacteria exhibited ~3 orders of magnitude increase in cell density, indicating uptake of diatom-
187 derived organic matter (Supplementary Fig. S3D). Surprisingly, co-cultures of *S. pseudonitzschiae* F5 with
188 *A. glacialis* showed a significant increase in longer diatom chains than axenic cultures, similar to
189 observations in xenic cultures (Supplementary Fig. S1C). This observation may be a byproduct of enhanced
190 growth of *A. glacialis* with *S. pseudonitzschiae* F5 or a result of a more complex mechanism of interaction.

191 *Sulfitobacter pseudonitzschiae* was first isolated from cultures of the toxigenic marine diatom *Pseudo-*
192 *nitzschia multiseries* obtained from the North Atlantic Ocean and the Pacific Northwest, with a model strain
193 first coined as *Sulfitobacter* sp. SA11 (Amin et al., 2015). Subsequently, several additional *S.*
194 *pseudonitzschiae* strains were isolated from the diatoms *Pseudo-nitzschia multiseries*, *Skeletonema marinoi*
195 and *A. glacialis* originating from the Atlantic Ocean, the Swedish coast, and the Persian Gulf, respectively
196 (Hong et al., 2015; Töpel et al., 2019). These repetitive recoveries of nearly identical bacteria (>99% 16S
197 rRNA sequence similarity) from three genera of diatoms that originated from starkly different locations
198 with large variations in temperature, salinity and nutrients indicate that *S. pseudonitzschiae* is a globally
199 distributed bacterium that may be a true symbiont of diatoms. *S. pseudonitzschiae* SA11 enhances the
200 growth rate of the diatom *P. multiseries* by 19-35% compared to axenic controls partially due to the activity
201 of the hormone IAA, which *S. pseudonitzschiae* biosynthesizes from diatom-derived tryptophan. Both

bioRxiv preprint doi: https://doi.org/10.1101/2020.07.26.221937; this version posted July 26, 2020. The copyright holder for this preprint (which was not certified by peer review) is the author/funder. All rights reserved. No reuse allowed without permission.

202 organisms also exchange organosulfur compounds and ammonia to complement each other's metabolism
203 (Amin et al., 2015). In this study, *S. pseudonitzschiae* F5 enhanced the growth rate of the diatom *A. glacialis*
204 by 27.6% (Supplementary Fig. S3C). Further genome sequencing and annotation showed that *S.*
205 *pseudonitzschiae* F5 also possesses three complete pathways for IAA biosynthesis from tryptophan
206 (Supplementary Table S1), suggesting it may use the same strategy as *S. pseudonitzschiae* SA11 to enhance
207 diatom growth.

208 Compared with *Sulfitobacter*, *Phaeobacter* species are known to colonize marine macro- and microalgal
209 surfaces (e.g., *Ulva australis*, *Thalassiosira rotula*) (Rao et al., 2006; Thole et al., 2012). *P. inhibens* has
210 been shown to control bacterial community assembly in the phycosphere of *T. rotula* (Majzoub et al., 2019).
211 *P. inhibens* also produces the hormone IAA to promote the growth of the coccolithophore, *Emiliania*
212 *huxleyi*, similar to *S. pseudonitzschiae* (Segev et al., 2016). *P. gallaeciensis* has been shown to lyse
213 senescent *E. huxleyi* by producing algicidal compounds known as roseobacticides (Seyedsayamdost et al.,
214 2011). Although *Phaeobacter* sp. F10 did not enhance the growth rate of *A. glacialis* (Supplementary Figure
215 S3B), metatranscriptomic analysis of a near-identical metagenomically assembled genome from the *A.*
216 *glacialis* strain A3 microbial consortium indicates that *Phaeobacter* sp. F10 is also a symbiont of *A.*
217 *glacialis* (Shibl et al., 2020).

218 Alteromonadaceae are widespread marine opportunistic copiotrophs (López-Pérez et al., 2012) that display
219 algicidal activities with phytoplankton during algal blooms (Mayali and Azam, 2004). The
220 *Pseudoalteromonas* and *Alteromonas* genera are known to effectively metabolize the organic matrix
221 surrounding diatom frustules, exposing the silica shell to increased dissolution by the surrounding water
222 (Bidle and Azam, 2001), and show strong algicidal activity by releasing dissolved substances (Mayali and
223 Azam, 2004). For example, *A. colwelliana* shows growth inhibition and algicidal activity against the diatom
224 *Chaetoceros calcitrans* (Kim et al., 1999). *A. macleodii* have been shown to degrade a variety of algal TEP

bioRxiv preprint doi: https://doi.org/10.1101/2020.07.26.221937; this version posted July 26, 2020. The copyright holder for this preprint (which was not certified by peer review) is the author/funder. All rights reserved. No reuse allowed without permission.

and exopolysaccharides (Koch et al., 2019) that may enable them to benefit from phytoplankton-derived carbon without contributing to phytoplankton metabolism. In addition, *A. macleodii* has been shown to compete for nitrate with the diatom *Phaeodacylum tricornutum* in the presence of organic carbon (Diner et al., 2016).

Bacterial attachment in the phycosphere

In order to test which bacterial strains attach to the diatom or TEP, we removed free-living bacterial cells from co-cultures of each strain with the diatom using gravity filtration through a 3-µm membrane filter and stained TEP with alcian blue, and diatom and bacterial nucleic acids with SYBR Green I (Fig. 1). Both symbiotic strains, *S. pseudonitzschiae* F5 and *Phaeobacter* sp. F10, displayed strong attenuation onto filters, while no attached *A. macleodii* F12 were observed (Fig. 1D-1F). The composite images of bright field and fluorescence showed a strong attachment preference to diatom TEP of *S. pseudonitzschiae* F5 and *Phaeobacter* sp. F10 in co-cultures with *A. glacialis* as observed in xenic cultures (Fig. 1G-1H). Surprisingly, *A. macleodii* F12 did not show any attachment capacity to *A. glacialis* or TEP (Fig. 1) despite its ability to degrade algal polysaccharides (Koch et al., 2019). These observations suggest an inherent mechanism that enables the roseobacters but not *A. macleodii* to attach to TEP. To shed more light on such mechanisms, we sequenced the genomes of all three isolates.

Genomic comparisons and AHLs identification

The genomes of the three strains were obtained by a combination of PacBio and Illumina sequencing as described in the methods. The GC contents of both *Roseobacter* group member genomes were more similar to each other (61.8% for *S. pseudonitzschiae* F5 and 60.0% for *Phaeobacter* sp. F10), while *A. macleodii* F12 had a lower GC content (44.9%) (Table 1), consistent with the phylogenetic similarities of *S. pseudonitzschiae* F5 and *Phaeobacter* sp. F10 compared to *A. macleodii* F12 (Supplementary Fig. S2). *S.*

bioRxiv preprint doi: https://doi.org/10.1101/2020.07.26.221937; this version posted July 26, 2020. The copyright holder for this preprint (which was not certified by peer review) is the author/funder. All rights reserved. No reuse allowed without permission.

pseudonitzschiae F5 possessed the largest estimated genome size (5.1 Mb) compared to *Phaeobacter* sp. F10 (4.0 Mb) and *A. macleodii* F12 (4.7 Mb) (Table 1). Consistent with this observation, *S. pseudonitzschiae* F5 also had the greatest number of predicted genes (4991) compared with either *Phaeobacter* sp. F10 (3878) or *A. macleodii* F12 (4654) (Supplementary Fig. S4A). A major difference between the three genomes was the apparent higher number of putative genes involved in membrane transport of substrates, particularly primary active transporters (e.g., amino acids, sugars) (Mishra et al., 2014). For example, the relative abundance of putative membrane transporters in the *S. pseudonitzschiae* F5 genome is 10.50% compared to *Phaeobacter* sp. F10 (8.44%) or *A. macleodii* F12 (7.05%) when normalized to genome size, with primary active transporters being the most abundant in the roseobacters' genomes but not in *A. macleodii* F12 (Supplementary Fig. S4B). This observation suggests that both symbionts are more attuned to phycosphere metabolites than *A. macleodii* F12.

Chemotaxis, motility, and attachment presumably contribute to successful colonization of phytoplankton surfaces. To examine the ability of all three bacteria to interact with the diatom phycosphere, we conducted a genome-wide analysis to compare genes involved in bacterial chemotaxis, motility, attachment, and quorum sensing. All three genomes contained four chemotaxis genes in a single operon-like structure (*cheA*, *cheR*, *cheW*, and *cheY*), while a fifth gene, *cheB*, was present in *Phaeobacter* sp. F10 and *A. macleodii* F12, but absent in *S. pseudonitzschiae* F5 (Fig. 2A and Supplementary Table S2). *CheAYW* together mediate a signal transduction cascade that functions to regulate flagellar motors, while *cheB* and *cheR* together regulate the methylation state of methyl-accepting chemotaxis proteins (Wuichet et al., 2007). Flagellar genes were present in all three genomes, although *S. pseudonitzschiae* F5 and *Phaeobacter* sp. F10 also contained a suite of flagellar structure genes absent in *A. macleodii* F12 (*flgN*, *fliG*, *flgJ*, *motB*, and MotA/TolQ/ExbB proton channel family protein). In addition, both *S. pseudonitzschiae* F5 and *Phaeobacter* sp. F10 contained 11 genes related to pilus formation in contrast to *A. macleodii* F12, which only contained a pilin *flp* gene, which is involved in pilus formation (Bardy et al., 2003). For attachment,

bioRxiv preprint doi: https://doi.org/10.1101/2020.07.26.221937; this version posted July 26, 2020. The copyright holder for this preprint (which was not certified by peer review) is the author/funder. All rights reserved. No reuse allowed without permission.

genes involved in exopolysaccharide production and biofilm formation were distributed throughout the genomes of the three bacteria (Fig. 2A and Supplementary Table S2). These lines of evidence suggest that *S. pseudonitzschiae* F5, *Phaeobacter* sp. F10, and *A. macleodii* F12 have the ability to carry out chemotaxis, construct flagella and pili structures, and form biofilm. Despite this observation, *A. macleodii* F12 did not attach to *A. glacialis* or TEP produced by *A. glacialis* (Fig. 1).

Quorum sensing (QS) autoinducers (e.g., AHLs) have been widely shown to modulate important biological functions, such as biofilm formation and motility (Bassler, 2002; Waters and Bassler, 2005), indicating QS may be able to regulate bacterial 'swim-or-stick' lifestyles in the phycosphere and suggesting that *A. macleodii* F12 may lack a functioning QS system. Indeed, *luxI*-like genes that are responsible for biosynthesizing AHLs were only present in *S. pseudonitzschiae* F5 (2 homologs) and *Phaeobacter* sp. F10 (1 homolog), while *A. macleodii* F12 completely lacked apparent *luxI* homologs (Fig. 2B and Supplementary Table S2). Indeed, *luxI* is rarely present in *Alteromonas* species. We found only two of 67 genomes belonging to the Alteromonadaceae that are publicly available contain putative AHL synthases. In addition to AHL synthesis, a transcriptional regulator, encoded by a *luxR* gene, is required to perceive AHLs and coordinate gene expression among bacterial populations. All three genomes contained *luxR* family genes, while *S. pseudonitzschiae* F5 possessed four putative *luxR*-family genes, *Phaeobacter* sp. F10 possessed six and *A. macleodii* F12 possessed only one (Fig. 2B and Supplementary Table S2). Typically, apparent *luxR* genes are found adjacent to or near a *luxI* gene on bacterial chromosomes in a single operon-like structure, such as in *S. pseudonitzschiae* F5 and *Phaeobacter* sp. F10 (Supplementary Table S2). However, some bacteria also have putative 'solo' *luxR* genes without associated putative *luxI* genes, which is the case in *A. macleodii* F12 and for the additional putative *luxR* homologs present in *S. pseudnonitzschiae* F5 and *Phaeobacter* sp. F10. It has been hypothesized that bacteria possessing 'solo' *luxR* genes do so to detect and respond to exogenous signals from other bacterial populations (Hudaiberdiev et al., 2015) or that these solo genes represent the loss of QS function (Subramoni and Venturi, 2009). Some

bioRxiv preprint doi: https://doi.org/10.1101/2020.07.26.221937; this version posted July 26, 2020. The copyright holder for this preprint (which was not certified by peer review) is the author/funder. All rights reserved. No reuse allowed without permission.

295 solo LuxR proteins have low specificity for AHL binding compared with LuxR proteins coupled with LuxIs
296 (Subramoni and Venturi, 2009). For example, SdiA, a solo transcriptional regulator that is present in
297 members of *Salmonella*, *Escherichia*, and *Klebsiella*, could bind seven different AHL molecules (Yao et
298 al., 2006; Janssens et al., 2007). Potentially, the solo *luxR* genes in *A. macleodii* F12 and the symbionts may
299 respond to a wide range of AHLs from other bacteria.

300 To characterize AHLs produced by *S. pseudonitzschiae* F5 and *Phaeobacter* sp. F10, we purchased a suite
301 of commercially available AHL standards (Supplementary Table S2) and used ultra-high-performance
302 liquid chromatography-tandem mass spectrometry (UHPLC-MS/MS) to identify potential AHLs in
303 bacterial cultures. Three AHLs were recovered from *S. pseudonitzschiae* F5 and *Phaeobacter* sp. F10 pure
304 culture supernatants with ionized parent masses of m/z 270.1700, 352.2480, and 354.2640 and identified
305 as 3-oxo-C_{10}-HSL, 3-oxo-$C_{16:1}$-HSL and 3-oxo-C_{16}-HSL, respectively, using high-resolution m/z values,
306 daughter-ion fragmentation and retention times (Fig. 3 and Supplementary Fig. S5). No standard from the
307 AHLs library matched any metabolite in the supernatant of *A. macleodii* F12, consistent with its lack of
308 *luxI*-like genes (Fig. 2). We attempted to measure AHLs in co-cultures of the roseobacters and the diatom
309 but due to the lower bacterial abundance in cocultures compared to pure bacterial cultures we were not
310 successful in detecting AHLs. The identification of AHL production by diatom symbionts prompted
311 examination of the influence of these signaling molecules on the ability of the symbionts to attach to diatom
312 TEP.

313 **Influence of AHLs on bacterial motility and biofilm formation**

314 Cell attachment is the first step in the process of biofilm formation, which requires motility for initial
315 attachment to surfaces (Slightom and Buchan, 2009). Consequently, we examined the influence of AHLs
316 on motility and biofilm formation since both functions are regulated by QS in bacteria (Hammer and Bassler,
317 2003; Daniels et al., 2004). All three AHLs and two QS inhibitors (QSIs), 2(*5H*)-furanone and furanone C-

bioRxiv preprint doi: https://doi.org/10.1101/2020.07.26.221937; this version posted July 26, 2020. The copyright holder for this preprint (which was not certified by peer review) is the author/funder. All rights reserved. No reuse allowed without permission.

30 (Ponnusamy et al., 2010; He et al., 2012), were used to test the motility and biofilm formation capabilities of *S. pseudonitzschiae* F5, *Phaeobacter* sp. F10, and *A. macleodii* F12. QSIs were used to confirm that any phenotypes observed using AHLs are due to QS regulation and not byproducts of other processes. Since the *A. macleodii* F12 genome contained a putative solo *luxR* gene (Fig. 2B), we suspected *A. macleodii* F12 might still respond to AHLs produced by *S. pseudonitzschiae* F5 and *Phaeobacter* sp. F10 despite lacking the ability to synthesize AHLs.

The addition of 2 μM of each AHL to each bacterium showed statistically significant inhibition of motility in *S. pseudonitzschiae* F5 and *Phaeobacter* sp. F10 ($p<0.01$) by all three AHLs, while both QSIs enhanced motility in *S. pseudonitzschiae* F5, as expected, and furanone C-30 enhanced motility in *Phaeobacter* sp. F10 (Fig. 4A and 4B). Specifically, 3-oxo-$C_{16:1}$-HSL exhibited the strongest inhibition of motility in *S. pseudonitzschiae* F5 by 78.2% ($p<0.001$) compared to the two other AHLs (28.6% and 31.8%). Despite showing two AHLs, 3-oxo-C_{16}-HSL and 3-oxo-C_{10}-HSL, weakly inhibiting motility in *A. macleodii* F12, both QSIs also weakly inhibited its motility, suggesting *A. macleodii* F12 does not respond or weakly responds to QS molecules (Fig. 4A and 4B). Bacterial motility is characterized by a circular swimming zone in the motility assay or by dendritic morphology, which is typical for swarming motility caused by a locally restricted movement on agar plates (Michael et al., 2016). *Phaeobacter* sp. F10 and *A. macleodii* F12 displayed a typical circular swimming zone while *S. pseudonitzschiae* F5 displayed a dendritic motility phenotype (Fig. 4A).

To assess biofilm formation, a standardized crystal violet assay was conducted as described previously (O'toole and Kolter, 1998). Interestingly, 10 μg/mL of 3-oxo-$C_{16:1}$-HSL significantly enhanced biofilm formation in *S. pseudonitzschiae* F5 and *Phaeobacter* sp. F10 by 26.7% and 211%, respectively ($p<0.05$), while 3-oxo-C_{10}-HSL and 3-oxo-C_{16}-HSL did not influence biofilm formation in either bacteria (Fig. 4C). These results suggest each AHL molecule regulates different sets of functions. Similar observations have

bioRxiv preprint doi: https://doi.org/10.1101/2020.07.26.221937; this version posted July 26, 2020. The copyright holder for this preprint (which was not certified by peer review) is the author/funder. All rights reserved. No reuse allowed without permission.

been shown previously (Su et al., 2018; Hou et al., 2019). In contrast, both QSIs inhibited biofilm formation of *S. pseudonitzschiae* F5 by 52.2% and 21.9%, respectively, relative to the control. None of the AHLs influenced biofilm formation of *A. macleodii* F12 (Fig. 4C).

These findings suggest that specific AHLs produced by diatom symbionts promote bacterial colonization of the phycosphere by enhancing bacterial capacity to form biofilms and reduce motility, both are functions essential to successfully colonize the phycosphere. In contrast, *A. macleodii* F12 is unable to respond to these molecules or to effectively attach to TEP. Other mechanisms must also be functioning to further prevent opportunists, like *A. macleodii* F12, from benefitting from diatom exudates. One such mechanism is the regulation of microbial consortia by the eukaryotic host, *A. glacialis*. *A. glacialis* has recently been shown to release the unusual metabolites, rosmarinic acid and azelaic acid, in the phycosphere in response to bacteria (Shibl et al., 2020). Azelaic acid promoted the growth of both symbionts and concomitantly inhibited the growth of *A. macleodii* F12. Similarly, rosmarinic acid inhibited the motility of *S. pseudonitzschiae* F5 and *Phaeobacter* sp. F10 in an identical way to 3-oxo-$C_{16:1}$-HSL, while upregulating motility in *A. macleodii* F12 (Shibl et al., 2020). Rosmarinic acid has been recently shown to interfere with QS in a plant pathogen (Hammer and Bassler, 2003), suggesting this molecule acts as a QSI. A similar mechanism of interfering with QS, a process known as quorum quenching, is used by the marine macroalga *Delisea pulchra* to inhibit swarming motility of *Serratia liquefaciens* by producing halogenated furanones (Rasmussen et al., 2000). Cumulatively, our observations suggest that *S. pseudonitzschiae* F5 and *Phaeobacter* sp. F10 switch their free-living mode to surface-attached mode to remain in the phycosphere by releasing AHLs. Combined with the diatom host release of unique secondary metabolites that further promote symbiont phycosphere colonization and inhibit colonization of opportunists, these mechanisms ensure diatoms are not prey to random encounters with opportunists and pathogens.

QS gene homology and organization in the *Roseobacter* group

bioRxiv preprint doi: https://doi.org/10.1101/2020.07.26.221937; this version posted July 26, 2020. The copyright holder for this preprint (which was not certified by peer review) is the author/funder. All rights reserved. No reuse allowed without permission.

To shed light on the prevalence of QS systems in the *Roseobacter* group, we constructed a phylogenetic tree of 52 sets of the LuxR-ITS-LuxI sequences (*luxRI* cassettes) in 32 *Roseobacter* group representative genomes. The tree revealed multiple conserved QS gene topologies that were distributed across the *Roseobacter* group (Fig. 5).

In Figure 5, half of the roseobacters genomes contained more than one pair of *luxRI* (18/31) and more than two AHL molecules were identified in nine strains. It has been shown that >80% of bacteria in the *Roseobacter* group possess at least one *luxRI* gene cassette (Buchan et al., 2016). *Phaeobacter* species consistently appear to produce more than three AHLs using 2−3 *luxI* homologs (Fig. 5 and Supplementary Table S3). For example, *Phaeobacter gallaeciensis* DSM 26640 produces up to 8 different AHLs via only three *luxI* homologs (Ziesche et al., 2015). Cude and Buchan (2013) provide a classification of the genetic makeup and organization of the *luxRI* gene cassettes and neighboring genes, with the B topology (B group) being the most common cassette structure (Fig. 5). In our work, B group contained 26 *luxRI* cassettes distributed in 26 genomes (Fig. 5). Both *S. pseudonitzschiae* F5 and *Phaeobacter* sp. F10 possess one cassette that belongs to this group, while a unique *luxRI* cassette only occurs in *S. pseudonitzschiae* F5. Interestingly, both *S. pseudonitzschiae* F5 and *Phaeobacter* sp. F10 strains produced the same three AHLs molecules (Fig. 3 and Supplementary Fig. S5), suggesting these molecules must be a byproduct of a homologous *luxI*, common to both *S. pseudonitzschiae* F5 and *Phaeobacter* sp. F10. This finding is consistent with previous studies showing that a single *luxI*-type gene is responsible for biosynthesizing more than one AHL molecule (Ortori et al., 2007; Hansen et al., 2015). LuxI proteins use S-adenosylmethionine (SAM) and acylated acyl-carrier protein (ACP) to catalyze the acylation and lactonization of AHL molecules (Churchill and Chen, 2011). Potentially, the *luxI* homolog common to *S. pseudonitzschiae* F5 and *Phaeobacter* sp. F10 does not discriminate well between different substrates and can accept acyl chains of varying lengths, enabling it to biosynthesize three AHLs. This lack of specificity could allow different AHL molecules produced by a single protein to bind different transcriptional

bioRxiv preprint doi: https://doi.org/10.1101/2020.07.26.221937; this version posted July 26, 2020. The copyright holder for this preprint (which was not certified by peer review) is the author/funder. All rights reserved. No reuse allowed without permission.

388 regulators and thus regulate different functions. By regulating the availability of substrates needed to make
389 each AHL, different AHLs may be produced depending on the environmental condition while continuously
390 expressing the same AHL synthase. For example, different temperatures have been shown to influence the
391 types and concentrations of seven different AHLs produced by one *luxI* in the fish pathogen *Aliivibrio*
392 *salmonicida* (Hansen et al., 2015). The diversity of substrates and selectivity levels of different *luxI*
393 homologs also influence the proportions of various AHLs produced by roseobacters (Ziesche et al., 2018).
394 *S. pseudonitzschiae* F5 and *Phaeobacter* sp. F10 were isolated from the same diatom, indicating horizontal
395 gene transfer may be responsible for their identical production of AHLs. The second *luxI* gene in *S.*
396 *pseudonitzschiae* F5 likely produces one or more other AHL molecules that we were not able to characterize
397 due to the limitation of AHL mass spectrometry standards. As mentioned before, *S. pseudonitzschiae* F5
398 displayed a dendritic motility phenotype, which is absent in most roseobacters (Bartling et al., 2018). It is
399 not clear what ecological advantage dendritic motility have on bacteria like *S. pseudonitzschiae*.
400 Interestingly, two additional *S. pseudonitzschiae* strains displayed this phenotype previously (Bartling et
401 al., 2018), indicating this phenotype is common in this species for unknown reasons.

402 The phycosphere is a unique environment that enables the accumulation of organic molecules in close
403 proximity to phytoplankton cells along with their associated bacterial populations. Mounting evidence
404 indicates that DOM secretions by phytoplankton lead to the accumulation of higher bacterial density in the
405 phycosphere when compared to bulk seawater (Blackburn et al., 1998; Smriga et al., 2016), which is the
406 ideal scenario under which QS systems are activated. The isolation sources of bacteria in Figure 5 indicate
407 that 37.5% of strains were isolated from a eukaryotic host and 21.9% from phytoplankton and that these
408 roseobacters produce a wide variety of long-chain AHLs (C_{10}-C_{18}) (Supplementary Table S3). Long-chain
409 AHLs are more stable in alkaline environments, such as the phycosphere, compared to short-chain AHLs
410 (Yates et al., 2002). Thus, the production of long-chain AHLs by roseobacters in the phycosphere may lead

bioRxiv preprint doi: https://doi.org/10.1101/2020.07.26.221937; this version posted July 26, 2020. The copyright holder for this preprint (which was not certified by peer review) is the author/funder. All rights reserved. No reuse allowed without permission.

411 to a higher local concentration than short-chain AHLs, and thus enable roseobacters to respond collectively
412 to the phycosphere environment more successfully than other bacteria.

413 Here, we have shown that two diatom symbionts use AHL molecules to inhibit their motility and enhance
414 biofilm formation, processes that likely control their ability to attach to diatom TEP and thus colonize the
415 phycosphere. In contrast, an opportunist bacterium was incapable of attaching to diatom TEP and was found
416 to lack the ability to synthesize AHL molecules. The advantage of symbionts to switch their lifestyle from
417 motile bacteria entering the phycosphere to permanent residents of this microenvironment is essential to
418 marine bacteria that rely on phycosphere exudates to survive. This 'swim-or-stick' switch appears also to
419 be partially controlled by diatoms that can make quorum sensing mimics, such as rosmarinic acid.
420 Significant work is needed to delineate the importance of bacterial intraspecies signaling vs eukaryotic host
421 interference in bacterial communication.

422

423 **Experimental procedures**

424 **Diatom growth**

425 *Asterionellopsis glacialis* strain A3 was deposited for this work in the National Center for Marine Algae
426 and Microbiota (NCMA) under the accession number CCMP3542. Axenic *A. glacialis* strain A3
427 (CCMP3542) was generated as described previously (Behringer et al., 2018). All diatom cultures were
428 grown at 22°C in a 12:12 hour light/dark diurnal cycle (125 µE m^{-2} s^{-1}) in semi-continuous batch cultures
429 (Brand et al., 1981). Since *in vivo* fluorescence linearly correlates with cell numbers during exponential
430 growth in batch cultures (Wood et al., 2005), diatom growth was monitored by measuring *in vivo*
431 fluorescence of chlorophyll *a* (relative fluorescence units, RFU) using a 10-AU fluorimeter (Turner Designs,
432 San Jose, CA, United States). Specific growth rates (μ) of diatoms were calculated from the linear regression

bioRxiv preprint doi: https://doi.org/10.1101/2020.07.26.221937; this version posted July 26, 2020. The copyright holder for this preprint (which was not certified by peer review) is the author/funder. All rights reserved. No reuse allowed without permission.

433 of the natural log of RFU versus time during the exponential growth phase of cultures. The standard
434 deviation of μ was calculated using values from biological replicates (n = 5 unless otherwise indicated) over
435 the exponential growth period. The relationship between cell density and RFU of *A. glacialis* strain A3 can
436 be formulated with the following equation: y = 14.958x - 0.519, where y is cells/µL and x is the RFU value,
437 calculated from the regression line of linear portion of the growth curve. The adjusted R^2 value for this
438 curve is 0.98 ($p < 0.001$).

439 **Bacterial isolation, identification and phylogenetic analysis**

440 To assess whether specific bacteria attach to *A. glacialis* strain A3, we cultivated bacteria from the xenic *A.*
441 *glacialis* strain A3 culture as described previously (Shibl et al., 2020). Briefly, bacteria were isolated from
442 the diatom at early stationary phase by serially diluting 0.5 mL 1000 times in sterile f/2 media (Guillard,
443 1975) and subsequently spreading 200 µL onto (1) marine agar plates, (2) plates containing per liter of
444 seawater: 15g agar and 2g carbon source (sodium succinate or glucose) and (3) sterilized *A. glacialis* strain
445 A3 culture suspension with 1.5% agar. Plates were incubated at 25°C in the dark for 3-7 days and single
446 colonies with unique morphologies were re-streaked 3 times to eliminate cross-contamination before
447 storage at -80°C in 15% glycerol stocks.

448 Bacterial isolates were identified using direct PCR (Hofmann and Brian, 1991). Isolates were incubated in
449 3 mL marine broth at 25°C in the dark until optical density (600 nm) reached 1.0; subsequently, 2 µL of
450 each bacterium was used as a DNA template in PCR. The 16S rRNA gene from all bacteria was amplified
451 by universal primers (27F, 1492R) as previously described (Amin et al., 2015). PCR products were purified
452 by the Wizard PCR purification kit (Promega) and sequenced using Sanger sequencing (Apical Scientific,
453 Malaysia). Sequences were aligned with 16S rRNA sequences from GenBank using ClustalW Multiple
454 Alignment in BioEdit 7.0.9.0. A neighbor-joining (NJ) phylogenetic tree was constructed with BIONJ
455 (Gascuel, 1997) using Kimura's two-parameter model. Another tree was constructed using the

bioRxiv preprint doi: https://doi.org/10.1101/2020.07.26.221937; this version posted July 26, 2020. The copyright holder for this preprint (which was not certified by peer review) is the author/funder. All rights reserved. No reuse allowed without permission.

Maximum Likelihood (ML) methods using PhyML 3.0 (Guindon et al., 2010) with GTR+R+I substitution model as determined by SMS (Lefort et al., 2017). The final 16S rRNA phylogenetic consensus tree was generated and edited using FigTree 1.4.2 (Rambaut, 2014). 16S rRNA of strains *S. pseudonitzschiae* F5, *Phaeobacter* sp. F10, and *A. macleodii* F12 were compared with the microbial community of *A. glacialis* recovered after 20 days of isolation from the field (Behringer et al., 2018) using the BLASTn tool in BLAST+ (Camacho et al., 2009).

Co-culture generation and growth

For co-cultures, axenic *A. glacialis* strain A3 was inoculated from an acclimated, mid-exponential phase growing culture into 25 mL sterile f/2 media to achieve an initial diatom cell density of ~4,000 cells/mL. Bacteria were grown in marine broth (ZoBell, 1941) in the dark overnight from a single colony at 26°C and shaking at 180 rpm. Cultures were centrifuged at 4000 rpm for 10 min followed by washing twice with sterile f/2 medium. Subsequently, cultures were used to inoculate axenic *A. glacialis* cultures at an initial bacterial density of ~1×10^4 cells/mL. Bacterial counts in co-cultures were quantified by staining 1 mL fresh bacterial cells with 1x SYBR Safe stain (Edvotek Corp. USA), incubating stained samples in the dark at room temperature for one hour and using a CyFlow Space flow cytometer (Partec, Münster, Germany). Specific growth rates of diatoms were calculated as described above. Specific growth rates (μ) of bacteria were calculated from the linear regression of the natural log of cell counts from 2-6 days of cultures. The standard deviation of μ was calculated using values from biological replicates (n = 3 unless otherwise indicated).

Bright-field and fluorescence microscopy

To observe transparent exopolymeric particles (TEP) distribution and their attached bacteria, two staining steps were applied. Alcian blue was first used to stain TEP in diatom cultures. 1 mL culture in mid-

bioRxiv preprint doi: https://doi.org/10.1101/2020.07.26.221937; this version posted July 26, 2020. The copyright holder for this preprint (which was not certified by peer review) is the author/funder. All rights reserved. No reuse allowed without permission.

478 exponential phase was gently filtered by gravity onto 3-µm 25 mm polycarbonate membrane filters
479 (Whatman) to remove free-living bacteria (~ 1 µm). Subsequently, 1 mL alcian blue in 0.06% glacial acetic
480 acid (pH 2.5) was allowed to gently run down the tube wall onto the filter to stain samples for 10 min at
481 room temperature (Long and Azam, 1996). Excess alcian blue was removed using a gentle wash with PBS
482 buffer and gently filtered by gravity. Subsequently, filters that only contained diatoms (~25 µm for a single
483 cell), TEP particles and attached bacteria were fixed with Moviol-Sybr Green I as described previously
484 (Lunau et al., 2005). Filters were visualized using a DMI6000B epifluorescence microscope (Leica) with a
485 DMC2900 color brightfield camera (Leica). Bright-field microscopy was used for TEP observation.
486 Fluorescence microscopy was used for bacteria and diatom nucleic acid observations. L5 fluorescence filter
487 was used for SYBR green I staining of both bacterial and algal nucleic acids with an excitation wavelength
488 range of 480 - 656 nm and an emission wavelength at 590 nm. Y5 fluorescence filter was used for algal
489 chlorophyll autofluorescence with the excitation wavelength of 620 nm and an emission wavelength of 700
490 nm. Both bright-field and fluorescence images were merged using LAS X software (Leica Microsystems,
491 Germany). The chain length of axenic, xenic *A. glacialis* strain A3 and co-culture of the diatom with *S.*
492 *pseudonitzschiae* F5 were quantified using an inverted microscope (Eclipse Ti-U, Nikon, Japan).

493 **Bacterial genome sequencing and assembly**

494 Genomic DNA of *S. pseudonitzschiae* F5, *Phaeobacter* sp. F10, and *A. macleodii* F12 were extracted from
495 pure bacterial cultures using an E.Z.N.A. Bacterial DNA Kit (Omega BIO-TEK) according to the
496 manufacturer's instructions. DNA yield and quality were measured and checked using a Qubit 3.0
497 Fluorometer (Invitrogen; Life Technologies) and gel electrophoresis.

498 Genome sequencing of all three bacterial genomes was conducted using the Illumina and PacBio platforms
499 at Apical Scientific Sdn. Bhd (Malaysia) for *S. pseudonitzschiae* F5 and *Phaeobacter* sp. F10 and at
500 Novogene (China) for *A. macleodii* F12. In brief, 100~1000 ng DNA was fragmented by acoustic disruption

bioRxiv preprint doi: https://doi.org/10.1101/2020.07.26.221937; this version posted July 26, 2020. The copyright holder for this preprint (which was not certified by peer review) is the author/funder. All rights reserved. No reuse allowed without permission.

using a Covaris S220 system (Covaris, Woburn, MA) for Illumina sequencing. Subsequently, DNA libraries were built using a NEBNext® Ultra ™ II DNA Library Prep Kit (NEB E7645S/L, New England BioLabs ® Inc.), and quantification and quality control of generated libraries were performed on an Agilent 2100 Bioanalyzer (Agilent Technologies, Santa Clara, CA). The libraries were then sequenced with TruSeq SBS Kit v4-HS reagents on an Illumina HiSeq 2500 platform (Illumina, San Diego, CA). For PacBio sequencing, DNA was sheared to ~15-20 kb using a Megarupter (Diagenode) and sequenced on a PacBio RS II system (Pacific Biosciences, Menlo Park, CA).

High-quality PacBio sub-reads were assembled by aligning the Illumina paired-end 150 bp reads with the Basic Local Alignment via Successive Refinement (BLASR) aligner, a tool that combines data from short read alignments with optimization methods from whole genome alignment (Chaisson and Tesler, 2012), and were trimmed using bbduk, aligned with bbmap, and the resulting sorted bam files and the Pacbio consensus reference were used as input to pilon (--genome genome.fasta, --bam input.bam) (Walker et al., 2014) for further error correction and polishing. The assemblies were further polished with arrow in Canu 1.7 with parameter corOutCoverage=60 (Koren et al., 2017). The largest circular contig in each assembly represented the chromosome size for each bacterium. In addition, plasmid contigs were BLASTed against closely related genomes to confirm these were indeed plasmids. For *S. pseudonitzschia* F5, we were not able to close the chromosome due to high number of repeats in the genome and thus exact chromosome size could not be determined (Table 1). The consensus reference was annotated by Prokka (Seemann, 2014) and RAST, and checked for completeness by BUSCO (Simão et al., 2015). Circa 1.2.1 (http://omgenomics.com/circa/) was used to draw chromosomes circos plot and chord diagram to compare the same gene locations in different genomes. All genome sequences and their annotations can be accessed at GenBank under the accession numbers WKFG01000000 and CP046140-CP046144.

bioRxiv preprint doi: https://doi.org/10.1101/2020.07.26.221937; this version posted July 26, 2020. The copyright holder for this preprint (which was not certified by peer review) is the author/funder. All rights reserved. No reuse allowed without permission.

Mining publicly available *Alteromonas* genomes for autoinducer synthase gene was performed on MicroScope (https://mage.genoscope.cns.fr/microscope/home/index.php). Identification and classification of transporter proteins in the three bacterial genomes was done using 6,097 membrane transport protein sequences downloaded from the Transporter Classification Database (TCDB) (Saier Jr et al., 2016). To this end, Gblast2 program (http://www.tcdb.org/labsoftware.php) with a cutoff e-value < $1e^{-20}$ was used and sequences with alignment scores <100 were removed. The chemotaxis, flagellar protein, pili, exopolysaccharides and quorum sensing related gene identities were confirmed by BLASTp with the model *Roseobacter* group strain *Ruegueria pomeroyi* DSS-3.

QS genes analysis

The *luxR*-like and *luxI*-like genes of *S. pseudonitzschiae* F5 and *Phaeobacter* sp. F10 were predicted by RAST and Prokka. Maximum likelihood phylogenetic trees of multiple copies of LuxI-like, genetically linked LuxR-like and their internal transcribed spacer (ITS) sequences from *S. pseudonitzschiae* F5, *Phaeobacter* sp. F10, and 30 publicly accessible *Roseobacter* group genomes were constructed using PhyML 3.0 (Guindon et al., 2010) with HKY85 substitution model, which was selected according to SMS (Smart Model Selection in PhyML) (Lefort et al., 2017). These 30 strains were chosen based on several criteria: 1) Strains must have published information about at least two AHLs molecules, motility and attachment lifestyles, 2) All strains have whole genomes publicly available, and one of the following two criteria: 3) Strains are phylogenetically related to *S. pseudonitzschiae* F5 and *Phaeobacter* sp. F10, or 4) Strains are well studied as model roseobacters. The *luxRI* and ITS sequences of *Pseudomonas aeruginosa* PAO1 (RefSeq accession number NC_002516.2) were used as an outgroup. Phylogeny was tested with a fast likelihood-based method aBayes (Anisimova et al., 2011) with 100 bootstraps.

AHLs extraction and identification

bioRxiv preprint doi: https://doi.org/10.1101/2020.07.26.221937; this version posted July 26, 2020. The copyright holder for this preprint (which was not certified by peer review) is the author/funder. All rights reserved. No reuse allowed without permission.

To extract AHL molecules, *S. pseudonitzschiae* F5 and *Phaeobacter* sp. F10 strains were re-plated from glycerol stocks and subsequently single picked colonies were inoculated overnight in 25-mL marine broth at 26°C in the dark and shaking at 180 rpm. Overnight cultures were subsequently transferred to 1 L sterile marine broth in triplicates and grown under the same conditions for 20 hours. Finally, bacterial cells were removed by centrifugation (15 min, 7000 rpm) when the optical density (600 nm) reached 1.0. To further remove residual bacteria, the supernatant was further filtered through 0.2-µm polycarbonate membrane filters (Whatman, NJ, United States). Oasis HLB solid-phase extraction (SPE) cartridges (3 cc, 540 mg) were activated according to the manufacturer's instructions and were subsequently used to remove organic molecules from the filtrates as previously described (Wang et al., 2017). Finally, extracts were eluted with 5 mL 0.1% (v/v) formic acid in methanol and dried using an evaporator (SpeedVac SC210A, Thermo Savant, Holbrook, NY, USA) and were stored at -20°C for subsequent UHPLC-MS/MS analysis. AHL standards (Supplementary Table S4) were acquired from Cayman Chemicals and Sigma-Aldrich in order to help identify AHLs from *S. pseudonitzschiae* F5 and *Phaeobacter* sp. F10.

AHLs were analyzed using an Agilent 1290 HPLC system coupled to a Bruker Impact II Q-ToF-MS (Bruker, Germany). Metabolites were separated using a reversed-phase separation method. In RP mode, medium-polarity and non-polar metabolites were separated using an Eclipse Plus C_{18} column (50mm × 2.1mm ID) (Agilent, US). Chromatographic separation consisted of MilliQ-H_2O + 0.2% formic acid (buffer A), and Acetonitrile + 0.2% formic acid (Buffer C) at a flowrate of 0.4 mL. The initial mobile phase composition was 90% A and 5% C followed by a gradient to 100% C over 18 min. The column was maintained at 100% C for 2 mins followed by cleaning with isopropanol for 3 min. The column was allowed to equilibrate for 4 min using the initial mobile phase composition. Detection was carried out in the positive ionization mode with the following parameters: Mass Range = 50 – 1300 m/z measured at 6 Hz, ESI source parameters: dry gas temperature = 220°C, dry gas flow = 10.0 l/min, Nebulizer pressure = 2.2 bar, Capillary V = 3000 V, end plate Offset: 500 V; MS-ToF tuning parameters: Funnel 1 RF = 150 Vpp, Funnel 2 RF =

bioRxiv preprint doi: https://doi.org/10.1101/2020.07.26.221937; this version posted July 26, 2020. The copyright holder for this preprint (which was not certified by peer review) is the author/funder. All rights reserved. No reuse allowed without permission.

200 Vpp, isCID Energy = 0 eV, Hexapole RF = 50 Vpp, Ion Energy = 4.0 eV, Low Mass = 90 m/z, Collision Energy = 7.0 eV, pre Pulse storage = 5 µs.

Data was processed and analyzed with Metaboscape 3.0 (Bruker, Bremen). Processing was conducted with the T-Rex3D algorithm with an intensity threshold of 500 and a minimum peak length of 10 spectra. Spectra were lock-mass calibrated, and features were only created if detected in a minimum of 3 samples. The presence of a specific AHL was determined by comparing the high-resolution parent ion mass, daughter ion masses and retention times of the purchased standards relative to bacterial extracts.

Bacterial motility and biofilm formation assays

Bacterial motility assay was performed using semisolid (0.25% w/v) marine agar plates supplemented with a final concentration of 2 µM of each AHL or QS inhibitor (QSI) as described previously (Zan et al., 2012). The QSIs 2(5*H*)-furanone and (*Z*-)-4-Bromo-5-(bromomethylene)-2(5*H*)-furanone (furanone C-30) were purchased from Sigma-Aldrich. *S. pseudonitzschiae* F5, *Phaeobacter* sp. F10, and *A. macleodii* F12 strains were grown in marine broth overnight, and then were gently inoculated using a sterilized toothpick into the center of the agar surface. Triplicate plates were incubated at 26°C for 3 days after which motility plates were observed using the Uvitec Cambridge Fire-reader imaging system. The proportion of motile area (percent motility) was measured using ImageJ software (http://rsb.info.nih.gov/ij/). Bacterial motility is characterized by a circular swimming zone in the motility assay or by dendritic morphology, which is typical for swarming motility caused by a locally restricted movement on agar plates (Michael et al., 2016).

Bacterial biofilm formation was quantified for *S. pseudonitzschiae* F5, *Phaeobacter* sp. F10, and *A. macleodii* F12 strains using the crystal violet assay (O'toole and Kolter, 1998). Briefly, bacteria were cultured in marine broth overnight and then diluted to ~1x10^5 cells/mL. 100 µL aliquots were transferred to a 96-well suspension culture plate (Greiner bio-one, CELLSTAR, Monroe, NC, USA). 10 µg/mL AHL

bioRxiv preprint doi: https://doi.org/10.1101/2020.07.26.221937; this version posted July 26, 2020. The copyright holder for this preprint (which was not certified by peer review) is the author/funder. All rights reserved. No reuse allowed without permission.

591 or QSI were added to each well respectively in triplicates as final concentration, which is optimized from
592 previous studies (Ren et al., 2001; Zhu et al., 2019) while controls received no AHL or QSI addition. The
593 plate was incubated at 26℃ for 24 h and subsequently 25 μL of 0.1% crystal violet was added to each well
594 and incubated at room temperature for 15 min. Wells were rinsed twice with 150 μL Milli-Q water to
595 remove free-living bacteria and then dried at 60℃ for 10 min. Finally, stained biomass was solubilized in
596 95% ethanol for 1 h and absorbance readings were measured using a plate reader (BioTek, Winooski, VT)
597 at 600 nm. Unpaired t-test was used to compare the significant differences of control and other variables in
598 bacterial swarming and biofilm formation.

bioRxiv preprint doi: https://doi.org/10.1101/2020.07.26.221937; this version posted July 26, 2020. The copyright holder for this preprint (which was not certified by peer review) is the author/funder. All rights reserved. No reuse allowed without permission.

Acknowledgements

We would like to thank the China Scolarship Council for the financial support of C.F. This research was partially carried out using the Core Technology Platforms resources at New York University Abu Dhabi. This work was funded by an NYU Abu Dhabi grant (AD179) to S.A.A.

Conflict of interest

The authors declare that they have no competing interests.

bioRxiv preprint doi: https://doi.org/10.1101/2020.07.26.221937; this version posted July 26, 2020. The copyright holder for this preprint (which was not certified by peer review) is the author/funder. All rights reserved. No reuse allowed without permission.

References

Abreu, P.C., Rörig, L.R., Garcia, V., Odebrecht, C., and Biddanda, B. (2003) Decoupling between bacteria and the surf-zone diatom *Asterionellopsis glacialis* at Cassino Beach, Brazil. *Aquatic microbial ecology* **32**: 219-228.

Amato, A., Sabatino, V., Nylund, G.M., Bergkvist, J., Basu, S., Andersson, M.X. et al. (2018) Grazer-induced transcriptomic and metabolomic response of the chain-forming diatom *Skeletonema marinoi*. *The ISME journal* **12**: 1594-1604.

Amin, S., Hmelo, L., Van Tol, H., Durham, B., Carlson, L., Heal, K. et al. (2015) Interaction and signalling between a cosmopolitan phytoplankton and associated bacteria. *Nature* **522**: 98-101.

Amin, S.A., Parker, M.S., and Armbrust, E.V. (2012) Interactions between diatoms and bacteria. *Microbiol Mol Biol Rev* **76**: 667-684.

Anisimova, M., Gil, M., Dufayard, J.-F., Dessimoz, C., and Gascuel, O. (2011) Survey of branch support methods demonstrates accuracy, power, and robustness of fast likelihood-based approximation schemes. *Systematic biology* **60**: 685-699.

Antunes, L.C.M., Ferreira, R.B., Buckner, M.M., and Finlay, B.B. (2010) Quorum sensing in bacterial virulence. *Microbiology* **156**: 2271-2282.

Bagatini, I.L., Eiler, A., Bertilsson, S., Klaveness, D., Tessarolli, L.P., and Vieira, A.A.H. (2014) Host-specificity and dynamics in bacterial communities associated with bloom-forming freshwater phytoplankton. *PLoS One* **9**.

Bar-Zeev, E., Berman-Frank, I., Girshevitz, O., and Berman, T. (2012) Revised paradigm of aquatic biofilm formation facilitated by microgel transparent exopolymer particles. *Proceedings of the National Academy of Sciences* **109**: 9119-9124.

Bardy, S.L., Ng, S.Y., and Jarrell, K.F. (2003) Prokaryotic motility structures. *Microbiology* **149**: 295-304.

Bartling, P., Vollmers, J., and Petersen, J. (2018) The first world swimming championships of roseobacters-Phylogenomic insights into an exceptional motility phenotype. *Syst Appl Microbiol* **41**: 544-554.

Bassler, B.L. (2002) Small talk: cell-to-cell communication in bacteria. *Cell* **109**: 421-424.

Behringer, G., Ochsenkühn, M.A., Fei, C., Fanning, J., Koester, J.A., and Amin, S.A. (2018) Bacterial communities of diatoms display strong conservation across strains and time. *Frontiers in microbiology* **9**: 659.

Bell, W., and Mitchell, R. (1972) Chemotactic and growth responses of marine bacteria to algal extracellular products. *The Biological Bulletin* **143**: 265-277.

Bertrand, E.M., McCrow, J.P., Moustafa, A., Zheng, H., McQuaid, J.B., Delmont, T.O. et al. (2015) Phytoplankton–bacterial interactions mediate micronutrient colimitation at the coastal Antarctic sea ice edge. *Proceedings of the National Academy of Sciences* **112**: 9938-9943.

Bidle, K.D., and Azam, F. (2001) Bacterial control of silicon regeneration from diatom detritus: significance of bacterial ectohydrolases and species identity. *Limnology and Oceanography* **46**: 1606-1623.

Blackburn, N., Fenchel, T., and Mitchell, J. (1998) Microscale nutrient patches in planktonic habitats shown by chemotactic bacteria. *Science* **282**: 2254-2256.

bioRxiv preprint doi: https://doi.org/10.1101/2020.07.26.221937; this version posted July 26, 2020. The copyright holder for this preprint (which was not certified by peer review) is the author/funder. All rights reserved. No reuse allowed without permission.

Bramucci, A.R., Labeeuw, L., Orata, F.D., Ryan, E.M., Malmstrom, R.R., and Case, R.J. (2018) The bacterial symbiont *Phaeobacter inhibens* shapes the life history of its algal host *Emiliania huxleyi*. *Frontiers in Marine Science* **5**: 188.

Brand, L.E., Guillard, R.R., and Murphy, L.S. (1981) A method for the rapid and precise determination of acclimated phytoplankton reproduction rates. *Journal of plankton research* **3**: 193-201.

Bruhn, J.B., Gram, L., and Belas, R. (2007) Production of antibacterial compounds and biofilm formation by *Roseobacter* species are influenced by culture conditions. *Appl Environ Microbiol* **73**: 442-450.

Buchan, A., LeCleir, G.R., Gulvik, C.A., and González, J.M. (2014) Master recyclers: features and functions of bacteria associated with phytoplankton blooms. *Nature Reviews Microbiology* **12**: 686-698.

Buchan, A., Mitchell, A., Cude, W.N., and Campagna, S. (2016) Acyl-homoserine lactone-based quorum sensing in members of the marine bacterial *Roseobacter* clade: complex cell-to-cell communication controls multiple physiologies. *Stress and Environmental Regulation of Gene Expression and Adaptation in Bacteria*: 225-233.

Burkhardt, B.G., Watkins-Brandt, K.S., Defforey, D., Paytan, A., and White, A.E. (2014) Remineralization of phytoplankton-derived organic matter by natural populations of heterotrophic bacteria. *Marine Chemistry* **163**: 1-9.

Camacho, C., Coulouris, G., Avagyan, V., Ma, N., Papadopoulos, J., Bealer, K., and Madden, T.L. (2009) BLAST+: architecture and applications. *BMC bioinformatics* **10**: 421.

Carvalho, C.C. (2018) Marine biofilms: a successful microbial strategy with economic implications. *Frontiers in Marine Science* **5**: 126.

Case, R.J., Labbate, M., and Kjelleberg, S. (2008) AHL-driven quorum-sensing circuits: their frequency and function among the Proteobacteria. *The ISME Journal* **2**: 345.

Chaisson, M.J., and Tesler, G. (2012) Mapping single molecule sequencing reads using basic local alignment with successive refinement (BLASR): application and theory. *BMC bioinformatics* **13**: 238.

Chi, W., Zheng, L., He, C., Han, B., Zheng, M., Gao, W. et al. (2017) Quorum sensing of microalgae associated marine *Ponticoccus* sp. PD-2 and its algicidal function regulation. *AMB Express* **7**: 1-10.

Churchill, M.E., and Chen, L. (2011) Structural basis of acyl-homoserine lactone-dependent signaling. *Chemical reviews* **111**: 68-85.

Cude, W.N., and Buchan, A. (2013) Acyl-homoserine lactone-based quorum sensing in the *Roseobacter* clade: complex cell-to-cell communication controls multiple physiologies. *Front Microbiol* **4**: 336.

Cude, W.N., Prevatte, C.W., Hadden, M.K., May, A.L., Smith, R.T., Swain, C.L. et al. (2015) *Phaeobacter* sp. strain Y4I utilizes two separate cell-to-cell communication systems to regulate production of the antimicrobial indigoidine. *Appl Environ Microbiol* **81**: 1417-1425.

Dang, H., Li, T., Chen, M., and Huang, G. (2008) Cross-ocean distribution of *Rhodobacterales* bacteria as primary surface colonizers in temperate coastal marine waters. *Appl Environ Microbiol* **74**: 52-60.

Daniels, R., Vanderleyden, J., and Michiels, J. (2004) Quorum sensing and swarming migration in bacteria. *FEMS Microbiology Reviews* **28**: 261-289.

Diner, R.E., Schwenck, S.M., McCrow, J.P., Zheng, H., and Allen, A.E. (2016) Genetic manipulation of competition for nitrate between heterotrophic bacteria and diatoms. *Frontiers in microbiology* **7**: 880.

bioRxiv preprint doi: https://doi.org/10.1101/2020.07.26.221937; this version posted July 26, 2020. The copyright holder for this preprint (which was not certified by peer review) is the author/funder. All rights reserved. No reuse allowed without permission.

Durham, B.P., Sharma, S., Luo, H., Smith, C.B., Amin, S.A., Bender, S.J. et al. (2015) Cryptic carbon and sulfur cycling between surface ocean plankton. *Proceedings of the National Academy of Sciences* **112**: 453-457.

Durham, B.P., Boysen, A.K., Carlson, L.T., Groussman, R.D., Heal, K.R., Cain, K.R. et al. (2019) Sulfonate-based networks between eukaryotic phytoplankton and heterotrophic bacteria in the surface ocean. *Nature microbiology* **4**: 1706-1715.

Field, C.B., Behrenfeld, M.J., Randerson, J.T., and Falkowski, P. (1998) Primary production of the biosphere: integrating terrestrial and oceanic components. *science* **281**: 237-240.

Franco, A.d.O.d.R., They, N.H., Canani, L.G.d.C., Maggioni, R., and Odebrecht, C. (2016) *Asterionellopsis tropicalis* (Bacillariophyceae): a new tropical species found in diatom accumulations. *Journal of phycology* **52**: 888-895.

Gardiner, M., Fernandes, N.D., Nowakowski, D., Raftery, M., Kjelleberg, S., Zhong, L. et al. (2015) VarR controls colonization and virulence in the marine macroalgal pathogen *Nautella italica* R11. *Frontiers in microbiology* **6**: 1130.

Gascuel, O. (1997) BIONJ: an improved version of the NJ algorithm based on a simple model of sequence data. *Molecular biology and evolution* **14**: 685-695.

Geng, H., and Belas, R. (2010) Molecular mechanisms underlying *Roseobacter*–phytoplankton symbioses. *Current opinion in biotechnology* **21**: 332-338.

Gram, L., Grossart, H.-P., Schlingloff, A., and Kiørboe, T. (2002) Possible quorum sensing in marine snow bacteria: production of acylated homoserine lactones by *Roseobacter* strains isolated from marine snow. *Appl Environ Microbiol* **68**: 4111-4116.

Guillard, R.R. (1975) Culture of phytoplankton for feeding marine invertebrates. In *Culture of marine invertebrate animals*: Springer, pp. 29-60.

Guindon, S., Dufayard, J.-F., Lefort, V., Anisimova, M., Hordijk, W., and Gascuel, O. (2010) New algorithms and methods to estimate maximum-likelihood phylogenies: assessing the performance of PhyML 3.0. *Systematic biology* **59**: 307-321.

Hammer, B.K., and Bassler, B.L. (2003) Quorum sensing controls biofilm formation in *Vibrio cholerae*. *Molecular microbiology* **50**: 101-104.

Hansen, H., Purohit, A.A., Leiros, H.-K.S., Johansen, J.A., Kellermann, S.J., Bjelland, A.M., and Willassen, N.P. (2015) The autoinducer synthases LuxI and AinS are responsible for temperature-dependent AHL production in the fish pathogen *Aliivibrio salmonicida*. *BMC microbiology* **15**: 69.

He, Z., Wang, Q., Hu, Y., Liang, J., Jiang, Y., Ma, R. et al. (2012) Use of the quorum sensing inhibitor furanone C-30 to interfere with biofilm formation by *Streptococcus mutans* and its *luxS* mutant strain. *International journal of antimicrobial agents* **40**: 30-35.

Hmelo, L.R., Mincer, T.J., and Van Mooy, B.A. (2011) Possible influence of bacterial quorum sensing on the hydrolysis of sinking particulate organic carbon in marine environments. *Environmental microbiology reports* **3**: 682-688.

Hofmann, M., and Brian, D. (1991) Sequencing PCR DNA amplified directly from a bacterial colony. *Biotechniques* **11**: 30-31.

bioRxiv preprint doi: https://doi.org/10.1101/2020.07.26.221937; this version posted July 26, 2020. The copyright holder for this preprint (which was not certified by peer review) is the author/funder. All rights reserved. No reuse allowed without permission.

Hong, Z., Lai, Q., Luo, Q., Jiang, S., Zhu, R., Liang, J., and Gao, Y. (2015) *Sulfitobacter pseudonitzschiae* sp. nov., isolated from the toxic marine diatom *Pseudo-nitzschia multiseries*. *International journal of systematic and evolutionary microbiology* **65**: 95-100.

Hou, H., Zhu, Y., Wang, Y., Zhang, G., and Hao, H. (2019) AHLs regulate biofilm formation and swimming motility of *Hafnia alvei* H4. *Frontiers in microbiology* **10**: 1330.

Huang, J.J., Han, J.-I., Zhang, L.-H., and Leadbetter, J.R. (2003) Utilization of acyl-homoserine lactone quorum signals for growth by a soil pseudomonad and *Pseudomonas aeruginosa* PAO1. *Appl Environ Microbiol* **69**: 5941-5949.

Hudaiberdiev, S., Choudhary, K.S., Vera Alvarez, R., Gelencsér, Z., Ligeti, B., Lamba, D., and Pongor, S. (2015) Census of solo LuxR genes in prokaryotic genomes. *Frontiers in cellular and infection microbiology* **5**: 20.

Janssens, J.C., Metzger, K., Daniels, R., Ptacek, D., Verhoeven, T., Habel, L.W. et al. (2007) Synthesis of N-acyl homoserine lactone analogues reveals strong activators of SdiA, the *Salmonella enterica* serovar Typhimurium LuxR homologue. *Applied and environmental microbiology* **73**: 535-544.

Jefferson, K.K. (2004) What drives bacteria to produce a biofilm? *FEMS microbiology letters* **236**: 163-173.

Kaczmarska, I., Mather, L., Luddington, I.A., Muise, F., and Ehrman, J.M. (2014) Cryptic diversity in a cosmopolitan diatom known as *Asterionellopsis glacialis* (Fragilariaceae): Implications for ecology, biogeography, and taxonomy. *American Journal of Botany* **101**: 267-286.

Karentz, D., and Smayda, T.J. (1984) Temperature and seasonal occurrence patterns of 30 dominant phytoplankton species in Narragansett Bay over a 22-year period (1959–1980). *Mar Ecol Prog Ser* **18**: 277-293.

Kazamia, E., Czesnick, H., Nguyen, T.T.V., Croft, M.T., Sherwood, E., Sasso, S. et al. (2012) Mutualistic interactions between vitamin B12 - dependent algae and heterotrophic bacteria exhibit regulation. *Environmental microbiology* **14**: 1466-1476.

Kim, J.H., Park, J.H., Song, Y.H., and Chang, D.S. (1999) Isolation and characterization of the marine bacterium, *Alteromonas* sp. SR-14 inhibiting the growth of diatom, *Chaetoceros* species. *Korean Journal of Fisheries and Aquatic Sciences* **32**: 155-159.

Koch, H., Dürwald, A., Schweder, T., Noriega-Ortega, B., Vidal-Melgosa, S., Hehemann, J.-H. et al. (2019) Biphasic cellular adaptations and ecological implications of *Alteromonas macleodii* degrading a mixture of algal polysaccharides. *The ISME journal* **13**: 92-103.

Kogure, K., Simidu, U., and Taga, N. (1981) Bacterial attachment to phytoplankton in sea water. *Journal of Experimental Marine Biology and Ecology* **56**: 197-204.

Koren, S., Walenz, B.P., Berlin, K., Miller, J.R., Bergman, N.H., and Phillippy, A.M. (2017) Canu: scalable and accurate long-read assembly via adaptive k-mer weighting and repeat separation. *Genome research* **27**: 722-736.

Korner, H. (1970) Morphologie und Taxonomie der Diatomeen-gattung *Asterionella*. *Nova Hedwigia* **20**: 557-724.

Labeeuw, L., Khey, J., Bramucci, A.R., Atwal, H., de la Mata, A.P., Harynuk, J., and Case, R.J. (2016) Indole-3-acetic acid is produced by *Emiliania huxleyi* coccolith-bearing cells and triggers a physiological response in bald cells. *Frontiers in microbiology* **7**: 828.

Lefort, V., Longueville, J.-E., and Gascuel, O. (2017) SMS: smart model selection in PhyML. *Molecular biology and evolution* **34**: 2422-2424.

bioRxiv preprint doi: https://doi.org/10.1101/2020.07.26.221937; this version posted July 26, 2020. The copyright holder for this preprint (which was not certified by peer review) is the author/funder. All rights reserved. No reuse allowed without permission.

764 Lewis, K. (2001) Riddle of biofilm resistance. *Antimicrobial agents and chemotherapy* **45**: 999-1007.

765 Long, R.A., and Azam, F. (1996) Abundant protein-containing particles in the sea. *Aquatic Microbial*
766 *Ecology* **10**: 213-221.

767 López-Pérez, M., Gonzaga, A., Martin-Cuadrado, A.-B., Onyshchenko, O., Ghavidel, A., Ghai, R., and
768 Rodriguez-Valera, F. (2012) Genomes of surface isolates of *Alteromonas macleodii*: the life of a
769 widespread marine opportunistic copiotroph. *Scientific reports* **2**: 696.

770 Lunau, M., Lemke, A., Walther, K., Martens-Habbena, W., and Simon, M. (2005) An improved method for
771 counting bacteria from sediments and turbid environments by epifluorescence microscopy.
772 *Environmental Microbiology* **7**: 961-968.

773 Majzoub, M.E., Beyersmann, P.G., Simon, M., Thomas, T., Brinkhoff, T., and Egan, S. (2019) *Phaeobacter*
774 *inhibens* controls bacterial community assembly on a marine diatom. *FEMS microbiology ecology* **95**:
775 fiz060.

776 Malviya, S., Scalco, E., Audic, S., Vincent, F., Veluchamy, A., Poulain, J. et al. (2016) Insights into global
777 diatom distribution and diversity in the world's ocean. *Proceedings of the National Academy of Sciences*
778 **113**: E1516-E1525.

779 Mayali, X., and Doucette, G.J. (2002) Microbial community interactions and population dynamics of an
780 algicidal bacterium active against *Karenia brevis* (Dinophyceae). *Harmful algae* **1**: 277-293.

781 Mayali, X., and Azam, F. (2004) Algicidal bacteria in the sea and their impact on algal blooms 1. *Journal of*
782 *Eukaryotic Microbiology* **51**: 139-144.

783 Mayali, X., Franks, P.J., and Burton, R.S. (2011) Temporal attachment dynamics by distinct bacterial taxa
784 during a dinoflagellate bloom. *Aquatic microbial ecology* **63**: 111-122.

785 Michael, V., Frank, O., Bartling, P., Scheuner, C., Goker, M., Brinkmann, H., and Petersen, J. (2016) Biofilm
786 plasmids with a rhamnose operon are widely distributed determinants of the 'swim-or-stick' lifestyle in
787 roseobacters. *ISME J* **10**: 2498-2513.

788 Miller, T.R., and Belas, R. (2004) Dimethylsulfoniopropionate metabolism by *Pfiesteria*-associated
789 *Roseobacter* spp. *Appl Environ Microbiol* **70**: 3383-3391.

790 Miller, T.R., and Belas, R. (2006) Motility is involved in *Silicibacter* sp. TM1040 interaction with
791 dinoflagellates. *Environmental microbiology* **8**: 1648-1659.

792 Miller, T.R., Hnilicka, K., Dziedzic, A., Desplats, P., and Belas, R. (2004) Chemotaxis of *Silicibacter* sp. strain
793 TM1040 toward dinoflagellate products. *Appl Environ Microbiol* **70**: 4692-4701.

794 Mishra, N.K., Chang, J., and Zhao, P.X. (2014) Prediction of membrane transport proteins and their
795 substrate specificities using primary sequence information. *PLoS One* **9**.

796 O'toole, G.A., and Kolter, R. (1998) Initiation of biofilm formation in *Pseudomonas fluorescens* WCS365
797 proceeds via multiple, convergent signalling pathways: a genetic analysis. *Molecular microbiology* **28**: 449-
798 461.

799 Ortori, C.A., Atkinson, S., Chhabra, S.R., Cámara, M., Williams, P., and Barrett, D.A. (2007) Comprehensive
800 profiling of N-acylhomoserine lactones produced by *Yersinia pseudotuberculosis* using liquid
801 chromatography coupled to hybrid quadrupole–linear ion trap mass spectrometry. *Analytical and*
802 *bioanalytical chemistry* **387**: 497-511.

bioRxiv preprint doi: https://doi.org/10.1101/2020.07.26.221937; this version posted July 26, 2020. The copyright holder for this preprint (which was not certified by peer review) is the author/funder. All rights reserved. No reuse allowed without permission.

803 Overhage, J., Lewenza, S., Marr, A.K., and Hancock, R.E. (2007) Identification of genes involved in
804 swarming motility using a *Pseudomonas aeruginosa* PAO1 mini-Tn5-lux mutant library. *Journal of*
805 *bacteriology* **189**: 2164-2169.

806 Pomeroy, L.R. (1974) The ocean's food web, a changing paradigm. *Bioscience* **24**: 499-504.

807 Ponnusamy, K., Paul, D., Kim, Y.S., and Kweon, J.H. (2010) 2 (*5H*)-Furanone: a prospective strategy for
808 biofouling-control in membrane biofilm bacteria by quorum sensing inhibition. *Brazilian Journal of*
809 *Microbiology* **41**: 227-234.

810 Raina, J.-B., Fernandez, V., Lambert, B., Stocker, R., and Seymour, J.R. (2019) The role of microbial motility
811 and chemotaxis in symbiosis. *Nature Reviews Microbiology* **17**: 284-294.

812 Rambaut, A. (2014) FigTree 1.4. 2 software. *Institute of Evolutionary Biology, Univ Edinburgh*.

813 Ramos, J.B., Schulz, K.G., Brownlee, C., Sett, S., and Azevedo, E.B. (2014) Effects of increasing seawater
814 carbon dioxide concentrations on chain formation of the diatom *Asterionellopsis glacialis*. *PloS one* **9**:
815 e90749.

816 Rao, D., Webb, J.S., and Kjelleberg, S. (2006) Microbial colonization and competition on the marine alga
817 *Ulva australis*. *Appl Environ Microbiol* **72**: 5547-5555.

818 Rasmussen, T.B., Manefield, M., Andersen, J.B., Eberl, L., Anthoni, U., Christophersen, C. et al. (2000) How
819 *Delisea pulchra* furanones affect quorum sensing and swarming motility in *Serratia liquefaciens* MG1.
820 *Microbiology* **146**: 3237-3244.

821 Ren, D., Sims, J.J., and Wood, T.K. (2001) Inhibition of biofilm formation and swarming of *Escherichia coli*
822 by (5Z)-4-bromo-5-(bromomethylene)-3-butyl-2 (*5H*)-furanone. *Environmental Microbiology* **3**: 731-
823 736.

824 Rodrigo-Torres, L., Pujalte, M.J., and Arahal, D.R. (2016) Draft genome of *Leisingera aquaemixtae* CECT
825 8399T, a member of the *Roseobacter* clade isolated from a junction of fresh and ocean water in Jeju Island,
826 South Korea. *Genomics data* **7**: 233-236.

827 Saier Jr, M.H., Reddy, V.S., Tsu, B.V., Ahmed, M.S., Li, C., and Moreno-Hagelsieb, G. (2016) The transporter
828 classification database (TCDB): recent advances. *Nucleic acids research* **44**: D372-D379.

829 Samo, T.J., Kimbrel, J.A., Nilson, D.J., Pett-Ridge, J., Weber, P.K., and Mayali, X. (2018) Attachment
830 between heterotrophic bacteria and microalgae influences symbiotic microscale interactions.
831 *Environmental microbiology* **20**: 4385-4400.

832 Seemann, T. (2014) Prokka: rapid prokaryotic genome annotation. *Bioinformatics* **30**: 2068-2069.

833 Segev, E., Wyche, T.P., Kim, K.H., Petersen, J., Ellebrandt, C., Vlamakis, H. et al. (2016) Dynamic metabolic
834 exchange governs a marine algal-bacterial interaction. *Elife* **5**: e17473.

835 Seyedsayamdost, M.R., Carr, G., Kolter, R., and Clardy, J. (2011) Roseobacticides: small molecule
836 modulators of an algal-bacterial symbiosis. *Journal of the American Chemical Society* **133**: 18343-18349.

837 Seymour, J.R., Amin, S.A., Raina, J.-B., and Stocker, R. (2017) Zooming in on the phycosphere: the
838 ecological interface for phytoplankton–bacteria relationships. *Nature microbiology* **2**: 17065.

839 Shibl, A.A., Isaac, A., Ochsenkühn, M.A., Cardenas, A., Fei, C., Behringer, G. et al. (2020) Diatom modulation
840 of microbial consortia through use of two unique secondary metabolites.
841 (https://doi.org/10.1101/2020.06.11.144840).

bioRxiv preprint doi: https://doi.org/10.1101/2020.07.26.221937; this version posted July 26, 2020. The copyright holder for this preprint (which was not certified by peer review) is the author/funder. All rights reserved. No reuse allowed without permission.

Simão, F.A., Waterhouse, R.M., Ioannidis, P., Kriventseva, E.V., and Zdobnov, E.M. (2015) BUSCO: assessing genome assembly and annotation completeness with single-copy orthologs. *Bioinformatics* **31**: 3210-3212.

Simon, N., Cras, A.-L., Foulon, E., and Lemée, R. (2009) Diversity and evolution of marine phytoplankton. *Comptes rendus biologies* **332**: 159-170.

Slightom, R.N., and Buchan, A. (2009) Surface colonization by marine roseobacters: integrating genotype and phenotype. *Appl Environ Microbiol* **75**: 6027-6037.

Smriga, S., Fernandez, V.I., Mitchell, J.G., and Stocker, R. (2016) Chemotaxis toward phytoplankton drives organic matter partitioning among marine bacteria. *Proceedings of the National Academy of Sciences* **113**: 1576-1581.

Spaepen, S., and Vanderleyden, J. (2011) Auxin and plant-microbe interactions. *Cold Spring Harbor perspectives in biology* **3**: a001438.

Spaepen, S., Vanderleyden, J., and Remans, R. (2007) Indole-3-acetic acid in microbial and microorganism-plant signaling. *FEMS microbiology reviews* **31**: 425-448.

Stocker, R. (2012) Marine microbes see a sea of gradients. *science* **338**: 628-633.

Su, Y., Tang, K., Liu, J., Wang, Y., Zheng, Y., and Zhang, X.-H. (2018) Quorum sensing system of *Ruegeria mobilis* Rm01 controls lipase and biofilm formation. *Frontiers in microbiology* **9**: 3304.

Subramoni, S., and Venturi, V. (2009) LuxR-family 'solos': bachelor sensors/regulators of signalling molecules. *Microbiology* **155**: 1377-1385.

Teeling, H., Fuchs, B.M., Becher, D., Klockow, C., Gardebrecht, A., Bennke, C.M. et al. (2012) Substrate-controlled succession of marine bacterioplankton populations induced by a phytoplankton bloom. *Science* **336**: 608-611.

Thole, S., Kalhoefer, D., Voget, S., Berger, M., Engelhardt, T., Liesegang, H. et al. (2012) *Phaeobacter gallaeciensis* genomes from globally opposite locations reveal high similarity of adaptation to surface life. *The ISME journal* **6**: 2229.

Thornton, D.C. (2014) Dissolved organic matter (DOM) release by phytoplankton in the contemporary and future ocean. *European Journal of Phycology* **49**: 20-46.

Töpel, M., Pinder, M.I., Johansson, O.N., Kourtchenko, O., Clarke, A.K., and Godhe, A. (2019) Complete genome sequence of novel *Sulfitobacter pseudonitzschiae* Strain SMR1, isolated from a culture of the marine diatom Skeletonema marinoi. *Journal of genomics* **7**: 7.

Van Mooy, B.A., Hmelo, L.R., Sofen, L.E., Campagna, S.R., May, A.L., Dyhrman, S.T. et al. (2012) Quorum sensing control of phosphorus acquisition in *Trichodesmium consortia*. *The ISME journal* **6**: 422-429.

Wagner-Döbler, I., and Biebl, H. (2006) Environmental biology of the marine *Roseobacter* lineage. *Annu Rev Microbiol* **60**: 255-280.

Walker, B.J., Abeel, T., Shea, T., Priest, M., Abouelliel, A., Sakthikumar, S. et al. (2014) Pilon: an integrated tool for comprehensive microbial variant detection and genome assembly improvement. *PloS one* **9**: e112963.

Wang, B., Tan, T., and Shao, Z. (2009) *Roseovarius pacificus* sp. nov., isolated from deep-sea sediment. *International journal of systematic and evolutionary microbiology* **59**: 1116-1121.

bioRxiv preprint doi: https://doi.org/10.1101/2020.07.26.221937; this version posted July 26, 2020. The copyright holder for this preprint (which was not certified by peer review) is the author/funder. All rights reserved. No reuse allowed without permission.

881 Wang, J., Ding, L., Li, K., Schmieder, W., Geng, J., Xu, K. et al. (2017) Development of an extraction method
882 and LC–MS analysis for N-acylated-l-homoserine lactones (AHLs) in wastewater treatment biofilms.
883 *Journal of Chromatography B* **1041**: 37-44.

884 Waters, C.M., and Bassler, B.L. (2005) Quorum sensing: cell-to-cell communication in bacteria. *Annu Rev*
885 *Cell Dev Biol* **21**: 319-346.

886 Windler, M., Bova, D., Kryvenda, A., Straile, D., Gruber, A., and Kroth, P.G. (2014) Influence of bacteria on
887 cell size development and morphology of cultivated diatoms. *Phycological Research* **62**: 269-281.

888 Wood, A.M., Everroad, R., and Wingard, L. (2005) Measuring growth rates in microalgal cultures. *Algal*
889 *culturing techniques* **18**: 269-288.

890 Wuichet, K., Alexander, R.P., and Zhulin, I.B. (2007) Comparative genomic and protein sequence analyses
891 of a complex system controlling bacterial chemotaxis. In *Methods in enzymology*: Elsevier, pp. 3-31.

892 Yao, Y., Martinez-Yamout, M.A., Dickerson, T.J., Brogan, A.P., Wright, P.E., and Dyson, H.J. (2006) Structure
893 of the *Escherichia coli* quorum sensing protein SdiA: activation of the folding switch by acyl homoserine
894 lactones. *Journal of molecular biology* **355**: 262-273.

895 Yates, E.A., Philipp, B., Buckley, C., Atkinson, S., Chhabra, S.R., Sockett, R.E. et al. (2002) N-acylhomoserine
896 lactones undergo lactonolysis in a pH-, temperature-, and acyl chain length-dependent manner during
897 growth of *Yersinia pseudotuberculosis* and *Pseudomonas aeruginosa*. *Infection and immunity* **70**: 5635-
898 5646.

899 Zan, J., Cicirelli, E.M., Mohamed, N.M., Sibhatu, H., Kroll, S., Choi, O. et al. (2012) A complex LuxR-LuxI type
900 quorum sensing network in a roseobacterial marine sponge symbiont activates flagellar motility and
901 inhibits biofilm formation. *Mol Microbiol* **85**: 916-933.

902 Zhu, Y.L., Hou, H.M., Zhang, G.L., Wang, Y.F., and Hao, H.S. (2019) AHLs regulate biofilm formation and
903 swimming motility of *Hafnia alvei* H4. *Frontiers in Microbiology* **10**: 1330-1330.

904 Ziesche, L., Rinkel, J., Dickschat, J.S., and Schulz, S. (2018) Acyl-group specificity of AHL synthases involved
905 in quorum-sensing in *Roseobacter* group bacteria. *Beilstein journal of organic chemistry* **14**: 1309-1316.

906 Ziesche, L., Bruns, H., Dogs, M., Wolter, L., Mann, F., Wagner‐Döbler, I. et al. (2015) Homoserine lactones,
907 methyl oligohydroxybutyrates, and other extracellular metabolites of macroalgae‐associated bacteria of
908 the *Roseobacter* Clade: Identification and functions. *ChemBioChem* **16**: 2094-2107.

909 ZoBell, C.E. (1941) Studies on marine bacteria. I. The cultural requirements of heterotrophic aerobes. *J*
910 *Mar Res* **4**: 42-75.

911

bioRxiv preprint doi: https://doi.org/10.1101/2020.07.26.221937; this version posted July 26, 2020. The copyright holder for this preprint (which was not certified by peer review) is the author/funder. All rights reserved. No reuse allowed without permission.

912 **Table 1.** Bacterial genome statistics.

Statistic	***S. pseudonitzschiae* F5**	***Phaeobacter* sp. F10**	***Alteromonas macleodii* F12**
Genome size (bp)	5,087,289	4,008,202	4,727,977
Number of contigs	17	3	5
Chromosome size (bp)	3,764,450*	3,783,964	3,117,849
CDs	4,991	3,878	4,654
GC content (%)	61.8	60.0	44.9
N50 value	179,155	153,588	3,122,272
L50 value	3	1	1

913 **S. pseudonitzschiae* F5 chromosome size estimation was not possible due to high level of repeats in the
914 genome. The size indicated is the size of the largest contig.

bioRxiv preprint doi: https://doi.org/10.1101/2020.07.26.221937; this version posted July 26, 2020. The copyright holder for this preprint (which was not certified by peer review) is the author/funder. All rights reserved. No reuse allowed without permission.

Figure legends

Fig. 1. Micrographs of *A. glacialis* strain A3 co-cultures with bacterial isolates. Diatom TEP were stained with alcian blue **(A, B, C)**. Diatom and bacterial DNA was stained with SYBR Green I **(D, E, F)**. Composite images show bacterial attachment mostly to TEP for *S. pseudonitzschiae* F5 and *Phaeobacter* sp. F10 but not *A. macleodii* F12 **(G, H, I)**. Background in light micrographs show membrane filters.

Fig. 2. Chromosomal maps of bacterial isolate genomes showing distribution and localization of loci involved in attachment, motility, chemotaxis and quorum sensing. Tracks from the outermost to the center represent position on each chromosome, forward-strand protein-coding genes, reverse-strand protein coding genes, rRNA and tRNA genes, GC content and GC skew, respectively. Chromosomes of *S. pseudonitzschiae* F5, *Phaeobacter* sp. F10, and *A. macleodii* F12 are color-labeled with red, blue and green, respectively. **(A)** Homologs related to chemotaxis, motility and attachment. **(B)** Homologs related to quorum sensing. Black line refers to a *luxI* gene homolog unique to *S. pseudonitzschiae* F5.

Fig. 3. Identification of acyl-homoserine lactones (AHLs) from roseobacters isolates. Structures and UHPLC–MS/MS chromatograms of AHLs of *S. pseudonitzschiae* F5 or *Phaeobacter* sp. F10 isolated from pure cultural supernatants compared to purchased standards. For complete MS/MS spectra refer to Supplementary Fig. S5.

Fig. 4. AHLs control bacterial motility and attachment in *Roseobacter* group bacteria. **(A)** Motility assays of *S. pseudonitzschiae* F5, *Phaeobacter* sp. F10 and *A. macleodii* F12 with three AHL molecules: 3-oxo-C_{10}-HSL, 3-oxo-C_{16}-HSL and 3-oxo-$C_{16:1}$-HSL, and two quorum sensing inhibitors (QSIs): 2(*5H*)-furanone and furanone C-30. Assays were conducted by inoculating 0.25% soft agar plates with each bacterium and incubating for three days. **(B)** Percent Motility of *S. pseudonitzschiae* F5, *Phaeobacter* sp. F10 and *A. macleodii* F12 in the presence of 2 µM AHLs or QSIs. **(C)** Biofilm quantification in the presence of 10

bioRxiv preprint doi: https://doi.org/10.1101/2020.07.26.221937; this version posted July 26, 2020. The copyright holder for this preprint (which was not certified by peer review) is the author/funder. All rights reserved. No reuse allowed without permission.

μg/mL AHLs or QSIs. Assays were conducted by incubating $1x10^6$ bacterial cells with each molecule in 96-well plates for 24 hours. Attachment was quantified using absorbance of solubilized crystal violet at 600 nm. All error bars represent standard deviation (S.D.) of triplicate experiments. * $p<0.05$, ** $p<0.01$, *** $p<0.001$).

Fig. 5. Maximum-likelihood phylogenetic tree of 50 LuxR-ITS-LuxI loci and neighboring genes in 32 roseobacterial genomes. Group B is highlighted by red branches at the top of the tree. Color shades indicate the different groups of luxR/I cassettes. Bacteria isolated in this study are bold-faced. Length shows the sequence length of LuxR-ITS-LuxI loci. D = dendritic motility, M = motility, A = attachment. Y and N indicate whether a bacterium is able or unable to carry out each function. Isolation origin of bacteria highlighted in red indicate a biological host origin. The number of AHL molecules reported from each bacterium is provided, if known. Note that information on which cassette makes which AHL molecule is scarce. Some bacteria are present twice in the tree because they possess more than one Lux-like operon. Gene neighborhood abbreviations: HK, histidine kinase; CHP, conserved hypothetical protein; TctA, TctA family transmembrane transporter; RND, RND multidrug efflux pump; AL, adenylosuccinate lyase; TF, trigger factor; Tran, transposase; TetR, TetR family transcriptional regulator; TR, transcriptional regulator. Bootstrap values >50% calculated from 1000 iterations are shown at branch nodes. *Full references are listed in Supplementary Information.

was not certified by peer review) is the author/funder. All rights reserved. No reuse allowed without permission.

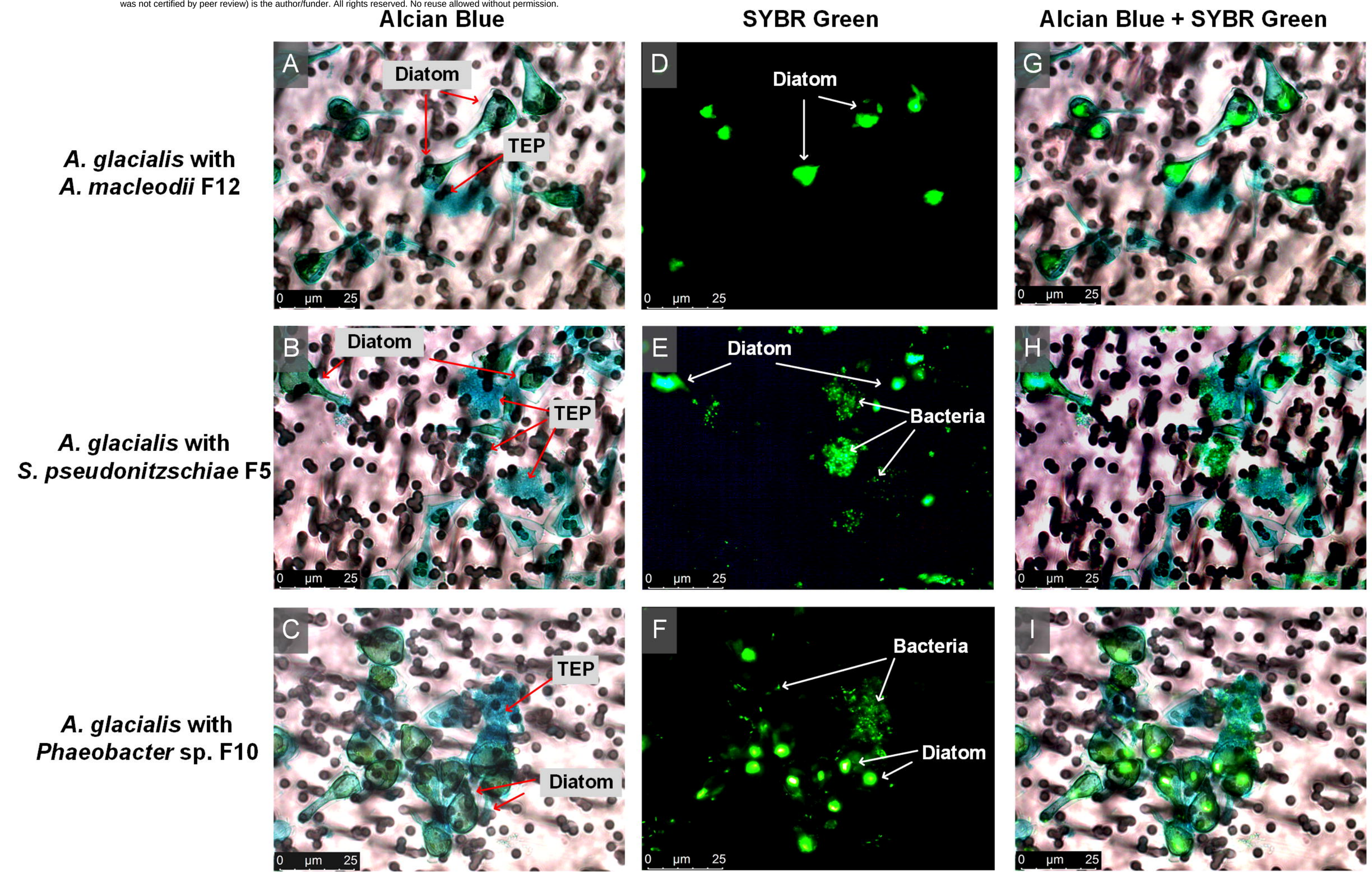

A

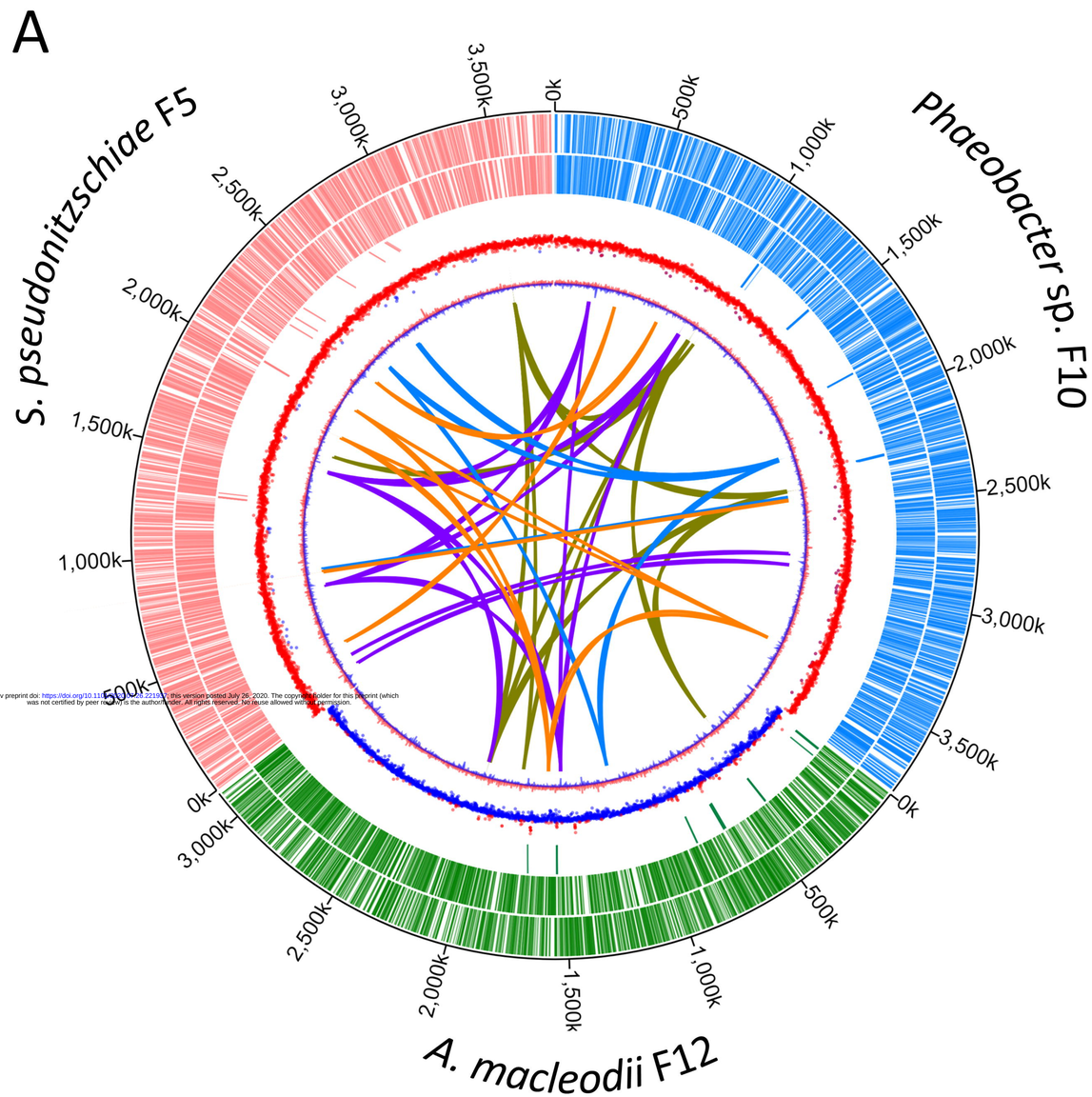

bioRxiv preprint doi: https://doi.org/10.1101/2020.07.26.221937; this version posted July 26, 2020. The copyright holder for this preprint (which was not certified by peer review) is the author/funder. All rights reserved. No reuse allowed without permission.

flagella gene pili gene

exopolysaccharide gene chemotaxis gene

B

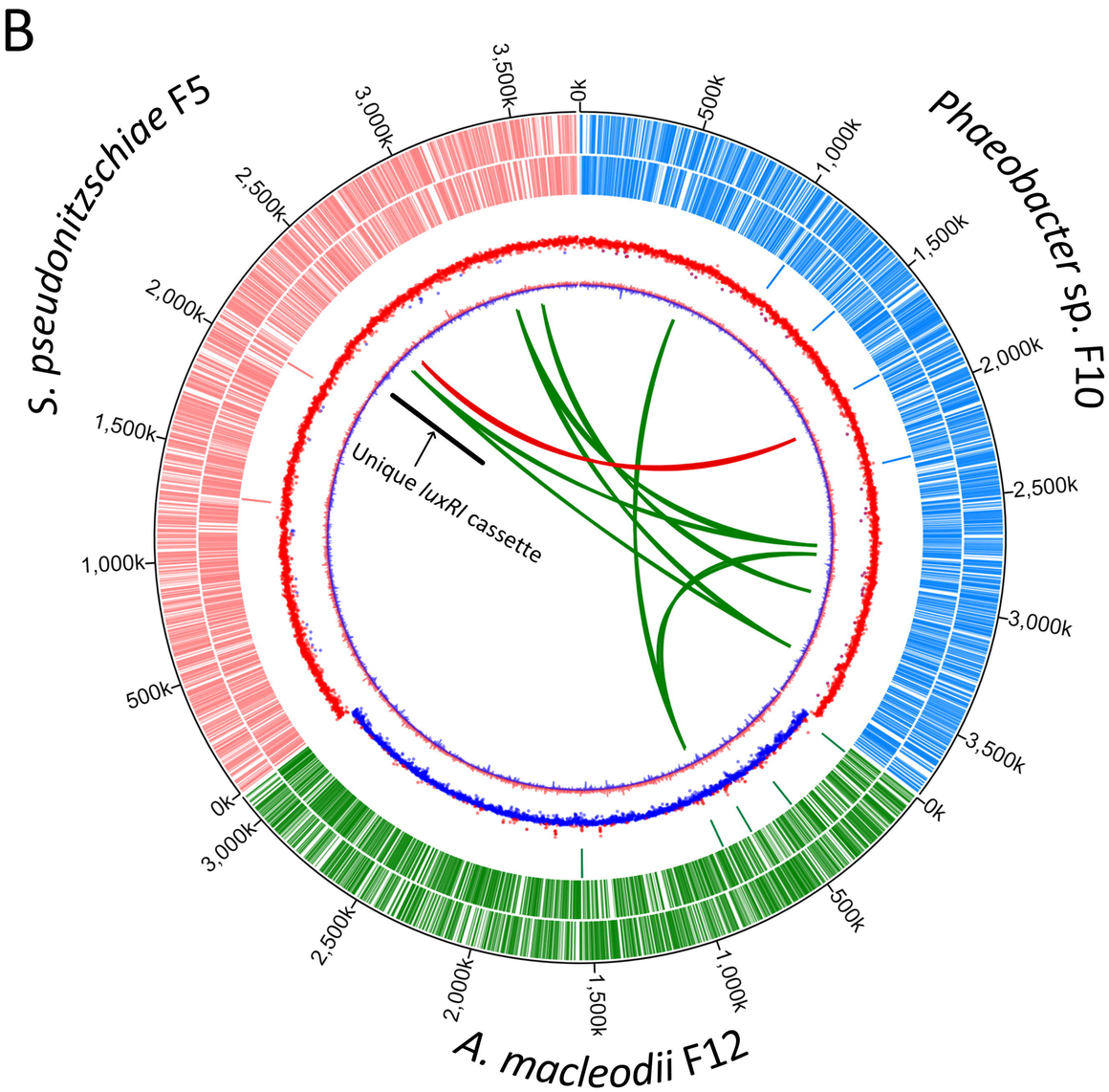

luxR family gene *luxRI* cassette

bioRxiv preprint doi: https://doi.org/10.1101/2020.07.26.221937; this version posted July 26, 2020. The copyright holder for this preprint (which was not certified by peer review) is the author/funder. All rights reserved. No reuse allowed without permission.

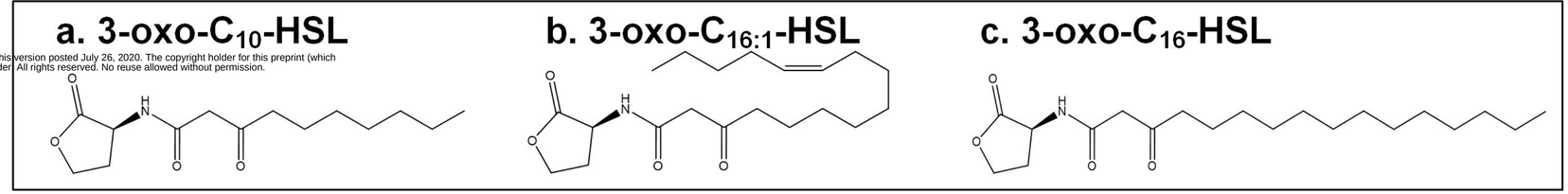

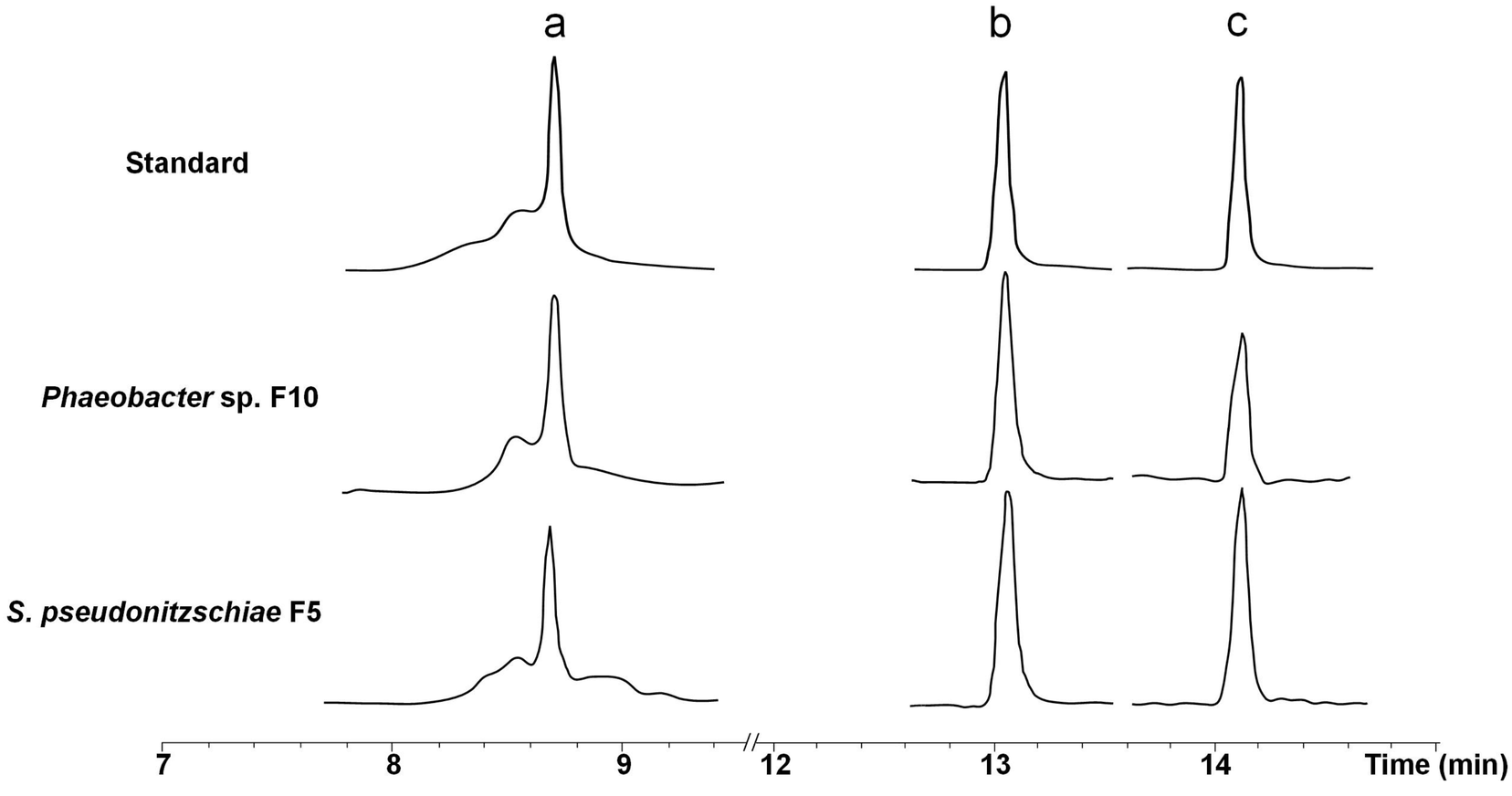

bioRxiv preprint doi: https://doi.org/10.1101/2020.07.26.221937, this version posted July 27, 2020. The copyright holder for this preprint (which was not certified by peer review) is the author/funder, who has granted bioRxiv a license to display the preprint in perpetuity. It is made available under a CC-BY-NC-ND 4.0 International license.

A

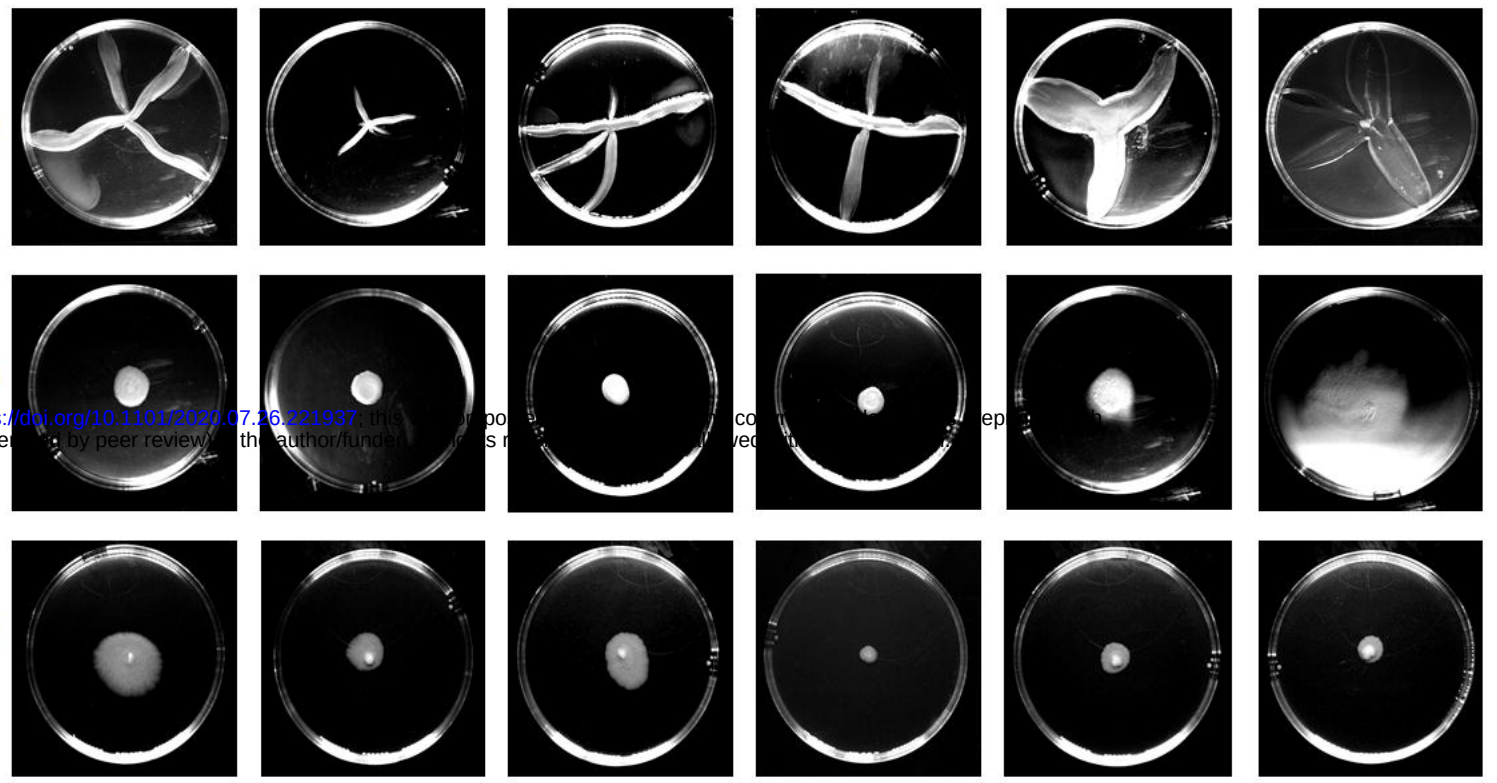

B

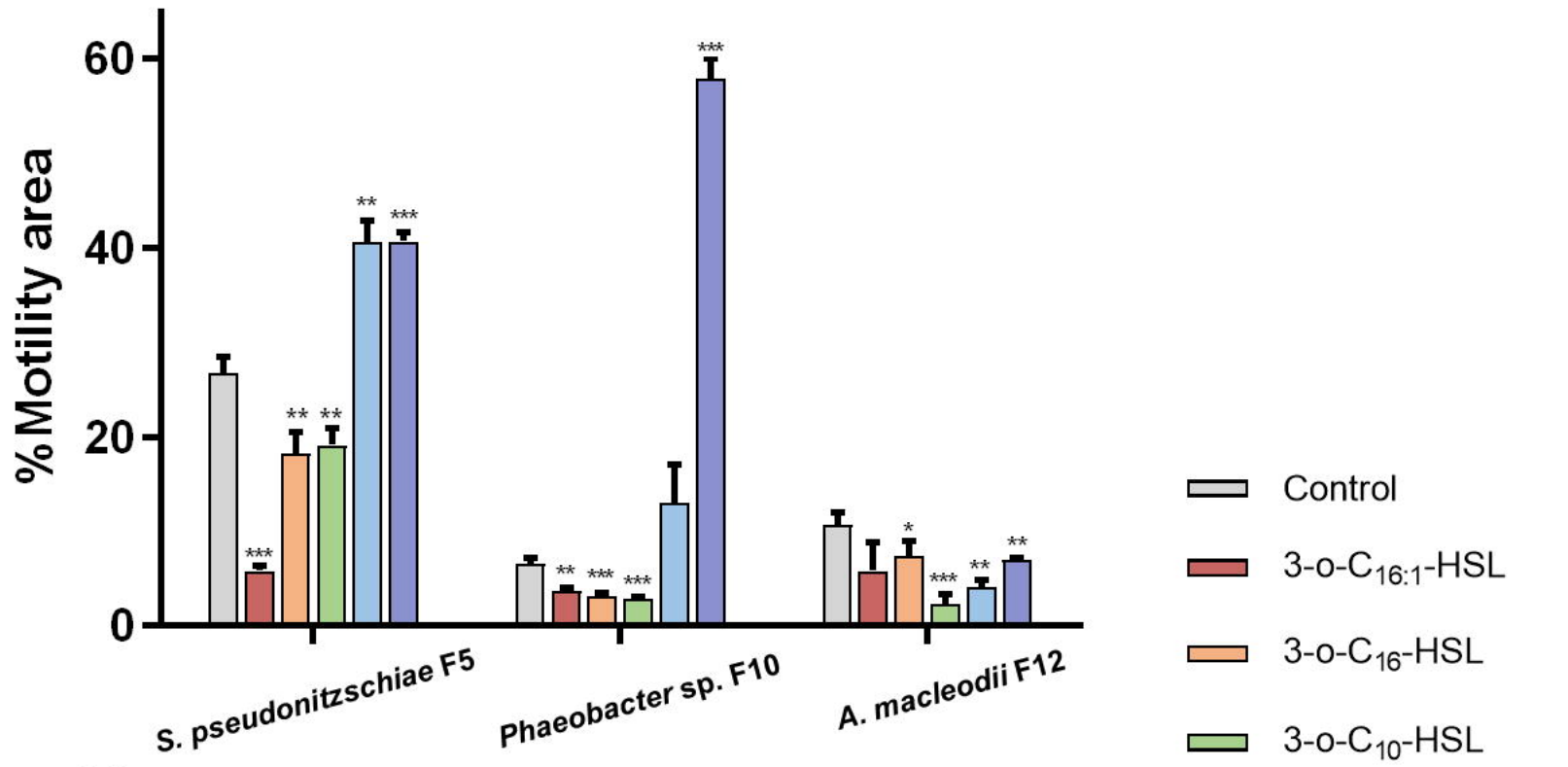

C

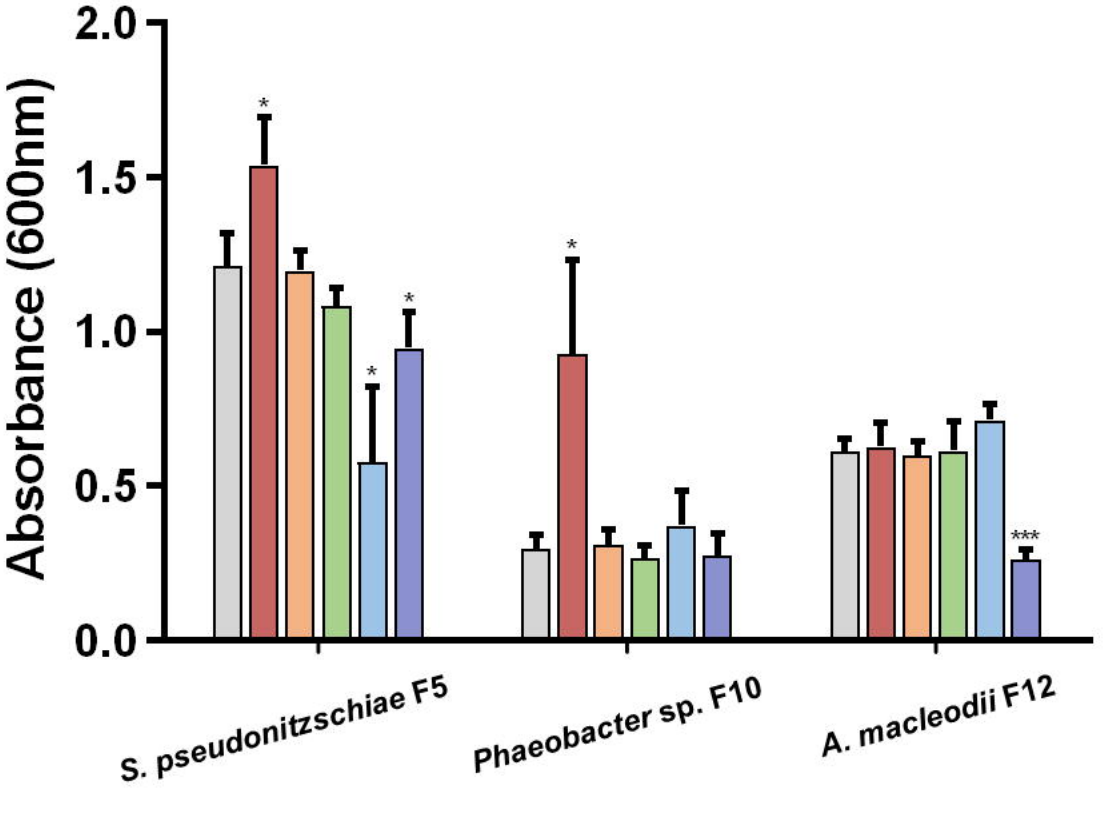

Autoinducer Synthase
AHL binding Response Regulator
Membrane protein
ATPase
Short chain dehydrogenase
Pyrimidine ABC transporter
L,D-transpeptidase ErfK/SrfK
Crotonyl-CoA reductase
HTH domain-containing protein

6.0

B group

Strains	1000bp Gene Clusters	Length (bp)	AHLs	Isolation source	M	A	References*
Phaeobacter sp. JL2872		1519		Surface seawater			
***Phaeobacter* sp. F10**		1473	3	***A. glacialis* (diatom)**	Y	Y	This study
Rhodobacterales bacterium Y4I		1714	2	Surface seawater	Y	Y	[1]
Leisingera sp. ANG1		1521		***E. scolopes* (squid)**			
Leisingera methylohalidivorans DSM 14336		1454		Surface seawater	Y	Y	[2]
Roseobacter sp. MED193		1490		Surface seawater			
Phaeobacter gallaeciensis DSM 26640		1456	8	**Scallop**	Y	Y	[3; 4]
Phaeobacter gallaeciensis DSM 17395		1456	4	**Scallop**	Y	Y	[5; 6]
Phaeobacter inhibens 2.10		1456	6	***U. australis* (green alga)**	Y	Y	[3; 5]
Ruegeria sp. R11		1455		***D. pulchra* (red algae)**	Y	Y	[7]
Ruegeria lacuscaerulensis ITI-1157		1462		Blue Lagoon in Iceland	N		[8]
Ruegeria sp. KLH11		1462	3	***M. laxissima* (marine sponge)**	Y	Y	[9]
Ruegeria pomeroyi DSS-3		1528	1	Surface seawater	N	N	[3]
Roseovarius pacificus 81-2		1577		Deep-sea sediment	D	Y	[10; 11]
Roseobacter sp. AzwK-3b		1447		Surface seawater			
Roseobacter sp. GAI101		1529		Surface seawater	Y		[9]
Rhodobacterales bacterium HTCC2150		1592		Surface seawater	N		[8]
Dinoroseobacter shibae DFL 12		1506	4	***P. lima* (dinoflagellates)**	N	N	[3;5]
Celeribacter marinus DSM100036		1464		Seawater	D		[10]
Sulfitobacter pseudonitzschiae DMS26824		1459		***P. multiseries* (diatom)**	D		[10]
***Sulfitobacter pseudonitzschiae* F5**		1459	3	***A. glacialis* (diatom)**	D	Y	This study
Sulfitobacter pseudonitzschiae SA11		1558		***P. multiseries* (diatom)**	D	Y	This study
Sulfitobacter sp. 20_GPM-1509m		1459		Deepwater			
Sulfitobacter pseudonitzschiae SMR1		1461		***S. marinoi* (diatom)**			
Roseobacter denitrificans Och 114		1582		Deep-sea sediment	N	N	[3]
Rhodobacteraceae bacterium PD-2		1534	2	***P. donghaiense* (dinoflagellates)**			
Rhodobacterales bacterium Y4I	HTH TctA	1460	2	Surface seawater	Y	Y	[8]
Leisingera methylohalidivorans DSM 14336	HTH PK	1354		Surface seawater	Y	N	[3]
Phaeobacter inhibens 2.10	HTH	1420	6	***U. australis* (green alga)**	Y	Y	[3; 5]
Phaeobacter gallaeciensis DSM 26640	CHP	2570	8	**Scallop**	Y	Y	[3; 4]
Phaeobacter sp. JL2872	TR Tran	2893		Surface seawater			
Roseobacter sp. MED193	Receptor CHP	2608		Surface seawater			
Roseobacter sp. AzwK-3b	HK	2284		Surface seawater	N		[8]
Sulfitobacter mediterraneus CH-B427	HK	753		Mediterranean Sea		N	[10]
Sulfitobacter pseudonitzschiae DMS26824	HK CHP CHP	774		***P. multiseries* (diatom)**	D		[10]
Sulfitobacter NAS-14.1	HK TetR RND	729		North Atlantic Ocean	Y		[8]
Sulfitobacter sp. EE-36	HK TetR RND	729		Salt marsh	Y	Y	[3; 12]
Roseobacter sp. CCS2	FliG AL	1408		Surface seawater	Y		[8]
Oceanicola granulosus HTCC2516	FliG AL	1521		Seawater	Y	Y	[3]
Phaeobacter gallaeciensis DSM 26640	CHP TR	1283	8	**Scallop**	Y	Y	[3; 4]
Rhodobacterales bacterium HTCC2150	TR CHP	1453		Surface seawater	N		[8]
Ruegeria lacuscaerulensis ITI-1157	CHP TF	1650		Blue Lagoon in Iceland	N		[8]
Ruegeria sp. KLH11	CHP TF	1801	3	***M. laxissima* (marine sponge)**	Y		[9]
Ruegeria pomeroyi DSS-3	HTH TF	1668	1	Surface seawater	N	N	[3]
Roseovarius pacificus 81-2	RP TF	1701		Deep-sea sediment	D		[10]
Rhodobacteraceae bacterium PD-2	Protease	1686	2	***P. donghaiense* (dinoflagellates)**			
Sulfitobacter pseudonitzschiae SA11		1503		***P. multiseries* (diatom)**	D	Y	This study
Sulfitobacter pseudonitzschiae DMS26824		1716		***P. multiseries* (diatom)**	D		[10]
***Sulfitobacter pseudonitzschiae* F5**		1716	3	***A. glacialis* (diatom)**	D	Y	This study
Sulfitobacter sp. 20_GPM-1509m		1716		Deepwater			
Sulfitobacter pseudonitzschiae SMR1		1632		***S. marinoi* (diatom)**			
Sulfitobacter NAS-14.1	CHP CHP	1517		North Atlantic Ocean	Y		[8]
Pseudomonas aeruginosa PAO1	P-type ATPase	1689	2	B. Holloway's collection	Y	Y	[13]

bioRxiv preprint doi: https://doi.org/10.1101/2020.07.26.221937; this version posted July 26, 2020. The copyright holder for this preprint (which was not certified by peer review) is the author/funder. All rights reserved. No reuse allowed without permission.